DMD Fast Forward. Published on June 19, 2008 as doi:10.1124/dmd.108.022566

Metabolism Distribution and Excretion of an MMP-13 Inhibitor CP-544439 in Rats and Dogs. Assessment of Metabolic Profile of CP-544439 in Plasma and Urine of Humans

Deepak Dalvie, Theresa Cosker, Tracey Boyden, Sue Zhou, Clinton Schroeder, and Michael J. Potchoiba

Pharmacokinetics, Dynamics and Metabolism Department, Pfizer Global Research and Development San Diego 92121 (DD, SZ), Groton Connecticut (TC, TB, CS and MJP)

Running Title: Disposition of CP-544439

Corresponding Author:

Deepak Dalvie, Ph. D.

Pharmacokinetics, Dynamics and Metabolism Department,

Pfizer Global Research and Development,

Science Center Drive, San Diego,

CA 92121.

E-mail: deepak.dalvie@pfizer.com,

Phone: (858) 622-8016.

Text pages: 54

Chart 1

Tables: 5

Figures: 8

Schemes: 3

References: 25

Words in Abstract: 248

Words in Introduction: 505

Words in Discussion: 1516

Abbreviations

MMP, Matrix metalloproteinase; UGT, Uridine diphosphoglucuronosyl transferase; PEG, polyethylene glycol; SD rats, Sprague-Dawley rats; WBAL, whole body autoradioluminography; GIT, Gastrointestinal tract; CP-544439 4-[4-(4-Fluorophenoxy)-benzenesulfonylamino]tetrahydropyran-4-carboxylic acid hydroxyamide.

Abstract

The metabolism and disposition of CP-544439 4-[4-(4-Fluorophenoxy)-benzenesulfonylamino]tetrahydropyran-4-carboxylic acid hydroxyamide a selective inhibitor of MMP-13, was investigated in rats and dogs following oral administration of [^{14}C]CP-544439. Both species showed quantitative recovery of the radiolabel and feces was the major route of excretion. Whole-body autoradioluminography study in rats suggested distribution of CP-544439 in all tissues except central nervous system. The radiolabel was rapidly eliminated from most tissues except the periodontal ligament. Metabolism of CP-544439 was extensive in both species. Only 8.4 and 1.5% of the total dose constituted unchanged CP-544439 in the rat and dog, respectively. Similarly, pharmacokinetic analysis of [^{14}C]CP-544439 and unchanged CP-544439 indicated that the exposure of the parent drug was 16 and 6.5% of the total radioequivalents in rat and dog, respectively. Metabolic profiling revealed that CP-544439 was primarily metabolized via glucuronidation, reduction and hydrolysis. Glucuronidation was the primary route of metabolism in dogs while reduction of the hydroxamate moiety was the major pathway in rats. Human plasma and urine obtained from a dose escalation study in healthy human volunteers were also analyzed in this study to assess the metabolism of CP-544439 in humans and ensure that selected animal species were exposed to all major metabolites formed in humans. Analysis suggested that CP-544439 was metabolized via all three pathways in humans consistent with rat and dog however, the glucuronide conjugate M1 was the major circulating and excretory metabolite in humans. Preliminary in vitro phenotyping studies indicated that glucuronide formation is primarily catalyzed by UGT1A1, 1A3 and 1A9.

The matrix metalloproteinases (MMP) are a family of zinc-dependent enzymes responsible for breaking down extracellular matrix proteins. Over-expression and activation of MMP has been linked to a range of diseases in which the destruction of connective tissue is an important pathological event such as osteo (OA) and rheumatoid (RA) arthritis, tumor metastasis and angiogenesis, and corneal ulceration (Michaelides and Curtin 1999; Beckett et. al., 1996; Rao, 2005). Collagenase 3 (MMP-13) is one type of MMP that is overexpressed in cartilage tissues of OA patients and is very efficient in the degradation of type II collagen. Thus MMP-13 has been implicated in the pathology of OA. A selective MMP-13 inhibitor should therefore slow down or prevent cartilage break down and improve the quality of life of OA patients by retarding loss of function due to joint deterioration.

CP-544439, 4-[4-(4-Fluorophenoxy)-benzenesulfonylamino]tetrahydropyran-4-carboxylic acid hydroxyamide (Chart 1), was designed and synthesized as a selective inhibitor of MMP-13 (IC_{50} = 0.8 nM) (Reiter et. al. 2004). In vivo studies using a hamster model, in which the cartilage collagen degradation was induced by intra-articular injection of recombinant human MMP-13 (Otterness et. al., 2000), demonstrated that oral administration of CP-544439 inhibits degradation of the cartilage collagen with an ED_{50} of 14 mg/kg and efficacious plasma concentrations ranging from 0.5 to 1.0 μg/mL. Preclinical pharmacokinetic studies of CP-544439 in rats and dogs demonstrated that the clearance of CP-544439 was high in rats (53 mL/min/kg) and moderate in dogs (10 mL/min/kg). The volume of distribution ranged from 1.6 to 2.0 L/kg in the two species and the terminal elimination half-life was 0.9 and 6.5 hr in rats and dogs, respectively (unpublished results). Pharmacokinetics of CP-544439 following single oral doses

ranging from 30 to 2000 mg to fasted healthy male human volunteers resulted in quantifiable plasma concentrations upto 12 to 24 hr depending on the dose (unpublished data). The systemic exposure of CP-544439, as assessed by C_{max} and $AUC_{0\text{-}tlast}$, increased proportionally with dose. The C_{max} ranged from 320 to 5200 ng/mL and $AUC_{0\text{-}Tlast}$ 650 to 25000 ng-hr/mL at these doses. The T_{max} ranged from 0.6 to 1.5 hr suggesting rapid absorption at all doses. The mean terminal elimination half-lives were short (1.6 to 2.6 hr) at all doses and were independent of dose escalation. Only a mean of 2.2% of the dose was excreted unchanged in the urine suggesting that CP-544439 was either eliminated unchanged in bile or extensively metabolized.

The primary objective of the present study was to investigate the metabolism, distribution and excretion of CP-544439 in rats and dogs (the toxicology species) following single oral administration of [^{14}C]CP-544439. Information generated from this study was used to suport the nonclinical safety evaluation of CP-544439. Since it is important to ensure that selected animal species are exposed to all major metabolites formed in humans (Baillie et. al. 2002; Hastings et. al. 2003), we also profiled the plasma and urine samples obtained from the dose escalation study that was conducted in healthy male human volunteers to assess the primary circulating and excretory metabolites of CP-544439 in humans.

Materials and Methods

General Chemicals. β-Glucuronidase (from Helix Pomatia, type H-1 with sulfatase activity), NADPH, UDPGA, human serum albumin (HSA) and α1-acid glycoprotein (AAG) were obtained from Sigma Chemical co. (St. Louis, MO). Carbosorb and Permafluor E+ scintillation cocktails were purchased from PerkinElmer Life and Analytical Sciences (Boston MA). HPLC-grade acetonitrile, methanol, water, ammonium formate and formic acid was purchased from Fischer Scientific Company (Springfield, NJ). Ecolite (+)scintillation cocktail was purchased from MP biomedicals (Solon, OH).

Radiolabeled Drug. [^{14}C]CP-544439 was synthesized at Vitrax, Placentia, CA and purified by the radiochemistry group at Pfizer Global Research (Groton, CT). The radiochemical purity was >99%, as determined by HPLC using an in-line detector and the specific activity was ~65 mCi/mmol.

Animal Studies. All experiments involving animals were carried out in compliance with national legislation and subject to local ethical review. Studies were conducted in a research facility accredited by the American Association for the Accreditation of Laboratory Animal Care. All study animals were acclimated to standard housing and environmental conditions in metabolism cages and rooms where light cycles, temperature and humidity were documented daily for 2 days before the experiments.

Rats: Three male and three female Sprague-Dawley (SD) rats were housed individually in Nalgene metabolism cages and fasted overnight. A single dose of [^{14}C]CP-544439 was administered orally at a target dose level of 250 mg/kg for a total radioactive dose of 112 μCi/kg and the specific activity of the dose was 0.455 μCi/mg. [^{14}C]CP-544439

was formulated in 0.1% methylcellulose:PEG 400 (1:1) until homogenous at a concentration of 50 mg/mL on the day of dose administration. Urine was collected from 0-8, 8-24, and at 24 hr intervals during the study and feces over 24 hr intervals, up to 168 hr post-dose. After the last urine and fecal collection, the cages were washed with 1:1 ethanol:water (v/v) and the wash was collected. The weight of each fecal sample, cage wash and the cage debris was determined. All animals were euthanized by CO_2 asphyxiation at the end of the study. For collection of bile, four Spraque Dawely rats (n= 2/ sex) were dosed orally with [^{14}C]CP-544439 at a dose of 250 mg/kg for a total radioactive dose of 118 μCi/kg and a specific activity of 0.472 μCi/mg. The dose was formulated in 0.1%methylcellulose/PEG400 to achieve a concentration of 25 mg/mL. Bile was collected from each animal from 0-4, 4-8, 8-24 hr post dose. Accurate measurements of bile volumes were noted for all time points. After sampling, the bile was stored at –4 °C until assayed. For pharmacokinetic studies, six Sprague Dawley rats (n = 3/sex) were dosed orally with 250 mg/kg [^{14}C]CP-544439 for a radioactive dose of 202 μCi/kg and a specific activity of 0.81 μCi/mg. The dose was formulated in 1:1 0.5% methylcellulose: PEG 400 to achieve a concentration of 25 mg/mL. Blood was collected pre-dose, 0.5, 1, 2, 4, 7, 25.5, 49.5, 57 and 72 hr post dose. After sampling, whole blood was centrifuged at 14000 rpm for 3 min, plasma transferred to eppendorf snap capped tubes and stored at –4 °C until assayed.

Dogs: Four non-cannulated (two per gender) and two bile-duct cannulated male Beagle dogs were housed individually in stainless steel metabolism cages. [^{14}C]CP-544439 was formulated at a target concentration of 20 mg/mL in 0.1% methylcellulose:PEG 400 (1:1) sonicated until homogenous. A single dose of [^{14}C]CP-544439 was administered

orally to each dog at a target dose level of 100 mg/kg. The specific activity of the dose was 0.080 μCi/mg. Each dog received a radioactive dose of 8 μCi/kg. Urine was collected from 0-8, 8-24, and then over 24 hr intervals and feces over 24 hr intervals, up to 168 hr post-dose during the study. Blood samples (5 mL) were collected and plasma was obtained prior to dosing and at 0.5, 1, 2, 4, 8, 12, 24, 48, 72 and 96 hr post dose. Bile was collected from the bile-duct cannulated animals up to 8 hr after dose. Cage debris was collected after each fecal collection and the cage floors, screens and pans were rinsed with aqueous ethanol (50%). After the last urine and fecal collection, the cages were washed with aqueous ethanol (50%) and the wash was collected.

Quantitation of Radioactivity. Radioactivity in the urine, bile and plasma was determined by liquid scintillation counting. Aliquots of plasma, urine and bile (50 -200 μL) were mixed with 15 to 20 mL Ecolite (+) scintillation cocktail counted in a Wallac Liquid Scintillation Counter Model 1409 (PerkinElmer Wallac, Turku, Finland). The fecal samples and the cage wash was placed in falcon tubes (50 mL) and homogenized in Milli-Q water into a thick slurry using a Binkmann Polytron lab homogenizer (Brinkmann Instruments, Westbury, NY). The total weight of the homogenate was recorded. Following homogenization, triplicate aliquots (200 μl) of each sample were transferred into tared cones and pads, weighed and combusted prior to radiometric analysis and allowed to dry at ambient temperature for 24 hr. All samples were combusted using a Model 307 sample oxidizer (PerkinElmer Life and Analytical Sciences, Boston, MA). The combustion efficiency was determined, prior to the combustion of the samples by using a carbon-14 standard. The resulting $^{14}CO_2$ was trapped in Carbo-Sorb® and mixed with Perma-Fluor V scintillation fluid and the radioactivity was quantified by liquid

DMD Fast Forward. Published on June 19, 2008 as DOI: 10.1124/dmd.108.022566
This article has not been copyedited and formatted. The final version may differ from this version.

scintillation counting. The measured radioactivity content in the samples was adjusted using the combustion efficiency values. The samples were analyzed for radioactivity in a Wallac Liquid Scintillation Counter for 2 min. All data obtained on the scintillation counter were automatically corrected for counting efficiency using external standardization technique. The samples obtained before dosing were also counted to obtain background count rate. Samples containing radioactivity (dpm) less than or equal to twice background for the system were assumed to contain zero dpm in the calculation of the means. The amount of radioactivity in the dose was expressed as 100% and the percentage of radioactivity in the urine and feces at each sampling time was expressed as the percentage of dose excreted in the respective matrices at the sampling time. The amount of radioactivity in the plasma was expressed as μg-equiv of CP-544439/mL and was calculated using the specific activity of the administered dose.

Quantitation of Unchanged CP-544439. The plasma samples were analyzed for unchanged CP-544439 using HPLC/tandem mass spectrometry. The internal standard (an analog of CP-544439; 20 μL of 2.5 μg/mL solution in acetonitrile) and 50 μL of 0.1% formic acid were added to 100 μL of the plasma sample and mixed thoroughly for 5 min. The analytes were extracted from the samples with methyl-tert-butyl ether (MtBE, 1.5 mL). The samples were vortexed for 5 min and the organic layer was separated by freezing the lower aqueous layer in a dry ice/acetone bath and then decanting the organic layers into fresh 15 x 100 ml conical glass tubes. The organic extract was evaporated to dryness under nitrogen at 50ºC. The sample residues were reconstituted in 100 μL of 70:30 water/acetonitrile prior to analysis. A 20 μL sample was injected on a system that consisted of Agilent quaternary HPLC pump with membrane degasser

(Agilent Technologies, Palo Alto, CA) and LEAP autosampler (CTC Analytics, LEAP Technologies Inc., NC) and was attached to a PE-Sciex API100 mass spectrometer (PerkinElmerSciex Instruments, Boston, MA) equipped with a Turbo ion Spray source. The internal standard and CP-544439 were separated chromatographically using a phenomenex C8 column (2.1 x 150 mm, 5 µm) analytical column at ambient temperature. The separation was carried out using 10 mM ammonium formate (pH 3) Solvent A, and acetonitrile Solvent B, as mobile phase and at a flow rate of 0.350 µL/min. The gradient system used was as follows: 20% solvent A from 0 to 5 min, changed from 20 to 90% solvent A from 5 to 30 min, kept at 90% solvent A from 30 to 34 min, changed from 90 to 20% solvent A over the next two min. The column was then allowed to equilibrate at 20% solvent A for the next 5 min before the next sample was injected. Compounds were detected in a negative ion mode, monitoring ions at *m/z* 409.1 and *m/z* 367.1 for CP-544439 and the internal standard, respectively. The retention times of CP-544439 and the internal standard were 18.7 and 16.6 minutes, respectively. Data collection and integration were done on Sciex Software Sample Control (version 1.4) and Mac Quan (version 1.6), respectively. The ratio of peak area responses of drug relative to internal standard was used to construct a standard curve using a linear least square regression with a $1/x^2$ weighting. The dynamic range of the assay was 0.01 to 2.0 µg/ml. The performance of the assay was monitored by inclusion of quality control samples prepared in rat or dog plasma from a separate weighing.

Determination of Pharmacokinetic Parameters: Pharmacokinetic parameters were determined by non-compartmental methods using WinNonLin version 2.1 (Pharsight, Mountain View, CA). The maximum plasma concentration (C_{max}) and the time at which

DMD Fast Forward. Published on June 19, 2008 as DOI: 10.1124/dmd.108.022566
This article has not been copyedited and formatted. The final version may differ from this version.

this concentration was achieved (T_{max}) were directly taken from the concentration data. The area under plasma concentration versus time curve ($AUC_{0\text{-}tlast}$) was calculated from 0 to the last quantifiable time point (T_{last}), using linear trapezoidal approximation. The plasma terminal elimination rate constant (k_{el}) was estimated by linear regression analysis of the terminal slope of log plasma concentration – time curve. The area from T_{last} to infinity (∞) was estimated by C_{tlast}/k_{el}, where C_{tlast} represented the estimated plasma concentration at T_{last}, based upon the aforementioned regression analysis. The area under the plasma concentration – time curve from zero to ∞ ($AUC_{0\text{-}\infty}$) was estimated as the sum of $AUC_{0\text{-}Tlast}$ and $AUC_{T\text{-}\infty}$.The terminal elimination half-life ($t_{1/2}$) was estimated as ln2/kel. For estimation of the means and pharmacokinetic parameters, concentrations at the 0 hr and those <0.010 μg/mL were assumed to be 0 μg/mL.

Extraction, Metabolic Profiling, Identification and Quantitation of Metabolites in Rat and Dog. Aliquots of plasma, bile and urine samples at various time points/animal were pooled relative to the excreted volume/mass at each time point, so that >90% of the radioactivity was accounted for. Pooled samples (0-72 hr, ~3 mL) from each animal were centrifuged and the supernatants were treated with acetonitrile (1:10) followed by a second centrifugation of the mixture. The supernatant was transferred to a glass conical tube and evaporated to dryness under nitrogen at 45°C in a Turbo-Vap (Caliper Life Sciences, Hopkinton, MA). Fecal homogenates at various sampling times were pooled on a weight basis to account for 90% of the radioactivity for each sample. Pooled samples (1 gm) were then treated with methanol (15 mL) and the mixture was vortexed and sonicated for about 60 min and then centrifuged at 3500 rpm. The

supernatants were separated and the process was repeated until most radioactivity (>90%) was recovered. All supernatants were mixed and evaporated to dryness under nitrogen in a Turbo-Vap at 45 ºC. All residues were reconstituted in 200 µl of acetonitrile:water mixture (1:3) and injected onto the HPLC column without further purification. An aliquot (25 µL) was injected onto the LC/MS.

Radiolabeled material in the reconstituted samples was profiled by reverse phase HPLC. The HPLC system consisted of an HP-1100 membrane degasser, HP-1100 autoinjector, HP-1100 binary gradient pump, and a radioactivity on-line detector fitted with a 100 µL YtHPSi solid scintillator flow cell (β-RAM; IN/US, Riviera Beach, FL). Chromatography was carried out on a Phenomenex C8 column (2.1 x 150 mm; 5 µm), Zorbax XDB C8 or a Eclipse-XDB fitted with Phenomenex C8 guard column utilizing a binary gradient of a mobile phase consisting of a mixture of 10 mM ammonium formate, pH 3.0 (Solvent A) and acetonitrile (Solvent B). The flow rate was 0.350 ml/min and the separation was achieved at ambient temperature. The gradient was 75% solvent A for the initial 12 min; ramped from 75 to 25% over 35 min in a linear fashion. It was then held at 25% for 1 min; then ramped to 90% in 1 min; held at 90% for 3 min and changed to 25% in 2 min. The column was then equilibrated at 75% A for the next 5 min before the next injection. The post-column eluate following injection of the extracts was split such that part of the flow was monitored continuously with a β-RAM online detector fitted with a 100 µl (INUS, Riviera Beach, FL. USA) at a flow rate of 275 µl/min. The remaining flow was diverted to the PE SCIEX API 3000 mass spectrometer for characterization of the metabolites. The mass spectrometer was operated in a negative ion mode and fitted with a turbo ionspray interface that was operated at an ionspray

voltage (IS) of -4000 V, orifice voltage (OR) of -36 V and a temprature of 200ºC. The collision induced dissociation (CID) studies (precursor ion scan or product ion scan) were performed using nitrogen gas at collision energy of 30 V and the collision gas thickness of 4 x 10^{14} molecules/cm^2. The data was analyzed by Sciex MultiView 1.4 software. Quantitation of metabolites was carried out by measuring radioactivity in the individually separated peaks in the radiochromatogram using Winflow software (IN/US, Riviera Beach, FL.). The post-column elute of rat and dog plasma and dog urine were generated by collecting fractions (Gilson Fraction Collector, FC-204, Middletown, WI) at 0.5-min intervals. Each fraction was mixed with scintillation cocktail (7 ml) and counting the fractions in a liquid scintillation counter. The counting efficiency was determined by external standardization. The counts (dpm) were plotted against time of fraction collection to obtain the plasma profile. The percentage of radioactivity for each peak was determined by dividing the number of counts in each peak by the total number of counts.

Enzymatic Hydrolysis. Pooled rat and dog bile samples (0.5 mL each) were adjusted to pH 5 with sodium acetate buffer (0.1 M) and treated with 10,000 units of β-glucuronidase from *Helix Pomantia* (Prakash and Soliman, 1997). The mixture was incubated in a shaking water bath at 37ºC for 12 hr. Control assays were run simultaneously under the same conditions without β-glucuronidase to estimate the stability of the glucuronide under such conditions. Incubations were quenched with acetonitrile (1:10), centrifuged and the supernatant was evaporated to dryness in a turbovap under nitrogen. The residue was reconstituted in 300 μL of acetonitrile and

water mixture (1:3) and 25 µl aliquot was injected onto the column for the identification of the glucuronide.

Microsomal Incubation of Metabolite M2 with Rat Liver Microsomes. Synthetic standard of the amide M2 (10 µM), was incubated with rat and dog liver microsomes (protein concentration 1.0 mg/mL), $MgCl_2$ (3.3 mM), and NADPH (3.0 mM) in a total volume of 1.0 mL potassium phosphate (0.1 M, pH 7.4). Incubations were started by addition of NADPH and shaken in a water bath set at 37°C for 30 min. At this time the incubations were quenched with acetonitrile (5 ml), centrifuged and the supernatant was evaporated to dryness in a Turbo-Vap under nitrogen. The residue was reconstituted in 150 µL of acetonitrile and water mixture (1:3) and 25 µL aliquot was injected onto the column for the identification of the oxidation products.

Metabolic Profiling of Human Plasma and Urine. Plasma and urine obtained was obtained from healthy human volunters dosed with 1000 mg of CP-544439 in the clinical pharmacology dose escalation study of CP-544439 was profiled to assess the circulating and urinary metabolites in humans. Aliquots (100 µL) of human plasma collected at 0.5, 1.0, 2.0, 4.0, 6.0, 12.0 and 16.0 hr were pooled per subject. Human urine samples collected from 0-6, 6-12 and 12-24 hr post dose/subject were pooled (1 mL/sampling time) into a single 0-24 hr sample for analysis. The pooled plasma and urine samples (1 mL) were treated with acetonitrile (5 mL) and the precipitated proteins were separated by centrifugation for 10 min at 2500 rpm. The supernatant was evaporated to dryness and the residue was reconstituted with 30% acetonitrile (100 µL) and vortexed. A 25 µL aliquot of the reconstituted mixture was then profiled by HPLC.

The separation was performed as described above except that an Eclipse-XDB column (2.1 x 150 mm; 5 μm) was used in the separation of metabolites. In the absence of the radiolabel, the effluent was directed into an UV detector (Hewlett Packard, Palo Alto, CA) which was set at a wavelength of 254 nm. The UV was recorded in real time by the mass spectrometer data system that provided simultaneous detection of UV and total ion chromatogram. No attempt was made to quantify the metabolites in the total ion chromatogram or in the UV chromatogram.

Plasma Protein Binding. The plasma protein binding experiment was conducted by equilibrium dialysis using Spectropor Equilibrium Dialysis System as described previously (Allan et. al. 2006). Fresh plasma was fortified with a methanol standard solution of [^{14}C]-CP-544439 (specific activity 64.98 mCi/mmol; radiochemical purity >99%) to yield a final concentration of 0.5, 1.0 and 2.5 μg/mL. For determination of CP-544439 binding to human serum albumin or α1-acid glycoprotein, fresh stock solution of human serum albumin (HSA, 45 mg/mL) and α1 acid glycoprotein (AAG, 0.75 mg/mL) in phosphate buffer (pH 7.4), was fortified with a methanol standard solution of [^{14}C]CP-544439 to yield a final concentration of 1.0 μg/mL. The 1.0 mL triplicate aliquots of fortified stock plasma, HSA and AAG were dialyzed against 1.0 mL Dulbecco's phosphate buffered saline (pH 7.4). The assembled dialysis cells were immersed in a water bath at 37°C and rotated at 20 rpm for ~16 hr. The total volumes of plasma and buffer samples were removed from the dialysis chambers with blunt needle syringes, and the corresponding volumes were measured to account for the volume shift during dialysis.

The plasma and buffer concentrations of CP-544439 were determined by liquid scintillation counting. An 100 mL aliquot of plasma and the buffer containing CP-544439 were mixed with scintillation cocktail (6 mL) and quantified in a Wallac liquid scintillation counter for 5 min. The counting efficiency was determined by external standardization. The unbound plasma free fraction was calculated by using the following formula:

$$fb = [(CPe - CBe)\cdot(VPe/VPi)]/\{[(CPe - CBe)\cdot(VPe/VPi)]\}+ CBe]$$

$$fu = 1-fb$$

fu = fraction unbound

fb = fraction bound

CPe = concentration of CP-544439 in plasma at equilibrium

CBe = concentration of CP-544439 in buffer at equilibrium

VPe = plasma volume at equilibrium

VPi = plasma volume at initial time point

Plasma Stability. CP-544439 was dissolved in methanol to provide a concentration of 0.1 mg/mL. To each 6 mL aliquot of rat, dog and human plasma, 60 μL of the 0.1 mg/mL solution of the CP-544439 were added to produce a final concentration in the incubation of 1.0 μg/mL. The fortified plasma was incubated in a water bath for 3 hr at 37ºC. A 500 μL aliquot was taken from each incubation upto 180 min and added to a

testube containing methyl tert-butyl ether (3 mL). The mixture was vortexed for 1 min and then centrifuged at 3000 rpm. The supernatant (organic layer) was dried in a turbo evaporator under nitrogen and the residue was reconstituted in a mixture of acetonitrile and water (30:70) and aliquot was analyzed by LC-MS/MS as described in the quantitation of CP-544439 section.

Whole-Body Autoradioluminography (WBAL) Study. Tissue distribution of [^{14}C]CP-544439 was investigated in six female and six male Long-Evans rats (Charles River Laboratories, Raleigh, NC) following oral administration. [^{14}C]CP-544439 was dissolved in 0.1% methyl cellulose:PEG 400 (1:1) mixture at concentration of 44.5 mg/mL and 49 μCi/mL. Specific activity of this dosing formulation was 0.46 mCi/mmol (1.1 μCi/mg). Delivery volumes were approximately 1 mL in order for each rat to receive 275 mg/kg and 302 μCi/kg of [^{14}C]CP-544439. [^{14}C]CP-544439 was orally administered to all rats. One rat of each gender was euthanized by CO_2 asphyxiation at 1, 3. 6, 18, 36 and 168 hr post dose. Immediately following euthanasia each rat was prepared for WBAL by immersion into a freezing chamber (-75ºC) containing dry ice and hexanes for 10 min.

The whole-body cryosectioning technique developed by Ullberg (Ullberg 1977) was used to acquire whole–body cryosections for autoradioluminography. Quantification of autoradioluminographic whole-body cryosection images as described by Potchoiba and co-workers was used to determine the radioactive concentrations of [^{14}C]CP-544439 in individual tissues, tissue substructures and gastro-intestinal (GIT) contents (Potchoiba et al., 1995, 1998). The lower limit of quantitation (LLOQ) for the WBAL assay was 3.3 nCi/g while the upper limit of quantitation (ULOQ) was 21,475 nCi/g. Tissue

concentrations of radioactivity (nCi/g) were converted to μg equivalents/g (μg eq/g) by using the specific activity of the [^{14}C]CP-544439 dose formulation. The pharmacokinetic parameters were calculated from mean tissue concentrations of radioactivity using WinNonLin ver. 2.1 (Pharsight, Mountain View, CA) as described above.

Identification of Uridine Glucuronyltransferase (UGT) Isoform Responsible for the Glucuronidation of CP-544439.

Microsomes prepared from baculovirus-infected insect cells that expressed the human UGTs 1A1, 1A3, 1A4, 1A6, 1A7, 1A8, 1A9,1A10, 2B4, and 2B7 (Supersomes), as well as a control preparation, were obtained from BD Biosciences (Billerica, MA). The glucuronidation activity of Supersomes from each UGT was substantiated by the supplier for the following substrates: estradiol (UGT 1A1 and 1A3), trifluoperazine (UGT 1A4), and 7-hydroxy-4-trifluoromethylcoumarin (UGT 1A6, 1A7, 1A8, 1A9, 1A10, 2B4, and 2B7).

Incubation Procedure: The typical incubation mixture (250 μL) contained Supersomes (1.0 mg/mL), $MgCl_2$ (10 mM), CP-544439 (20 μM) and alamethicin (25 μg/mg protein) in phosphate buffer (100 mM, pH 7.4). The supersomes were preincubated at 37ºC for 5 min and the reaction was started by addition of UDPGA (5 mM). After 60 min of incubation at 37°C, the reaction was stopped by addition of 150 μL of acetonitrile containing 50 μM internal standard. After centrifugation at 3000 rpm, 100 μL supernatant was transferred to a 1.5 mL marsh tube and diluted with 50 μL of acetonitrile and water (70:30). Control incubations without microsomes or without co-substrates were performed in parallel. All samples were analyzed by HPLC-MS system

that comprised of PE-Sciex 4000 mass spectrometer fitted with a turbo ion-spray, a Shimadzu system controller and pumps SCL-10A*VP* (Shimadzu Scientific Instruments, Columbia, MD), a Leap autosampler (CTC Analytics, LEAP Technologies Inc., Carrboro, NC). Samples (20 μL) were injected onto a Phenomenex Synergi Hydro-RP column (30 x 4.6 mm 4 μm, Phenomenex, Torrance, CA) preequilibrated with 0.1% formic acid solution in water, pH 3 (Solvent A) and acetonitrile containing 0.1% formic acid (Solvent B) at 90:10. The separation of the analytes was accomplished by using a gradient that comprised Solvent A at 90% up to 0.3 min that was changed to Solvent A at 10% from 0.3 to 0.5 min. The Solvent A was then maintained at 10% from 0.5 to 2.30 min and changed to 90% in the next 0.2 min. It was then allowed to equilibrate for 0.5 min between sample injections. The flow rate was maintained at 300 μL/min. Detection was accomplished in the positive ion mode on a Sciex 4000, monitoring the metabolite at *m/z* 587 to 411 and the internal standard at *m/z* 272.5 to 135.2, respectively. The tune file settings on the mass spectrometer were as follows; source temperature 400ºC, declustering potential (DP) 41; collision energy (CE) 15 (for the conjugate) and 61 (for the internal standard). The retention time for M1 and the internal standard were 1.3 and 1.4 min respectively. The peak areas of the conjugate and the internal standard were processed by Sciex Software Analyst 1.4. Since the synthetic standard of the glucuronide conjugate was not available the ratio of peak area responses of the conjugate relative to internal standard was used to determine the abundance of the conjugate fromed by each isoform.

Results

Pharmacokinetics

All studies were conducted using doses that mimicked the tolerated intermediate doses used in toxicology studies. Hence the ADME study in the rat was conducted at 250 mg/kg dose whereas the study in the dog was conducted at 100 mg/kg dose.

Rat: The mean plasma concentration versus time profile for total radioactivity (µg-equiv. unchanged CP-544439/mL) and unchanged CP-544439 (µg/mL) following single oral administration of [^{14}C]CP-544439 to rat and dog is shown in Figure 1. The pharmacokinetic parameters are depicted in Table 1. After an oral dose of 250 mg/kg of [^{14}C]CP-544439 to SD rats, the mean C_{max} of total circulating radioactivity and unchanged CP-544439 was 24.0 µg-equiv of CP-544439/mL and 12.7 µg/mL, respectively, and the mean T_{max} was 8.0 hr and 2.2 hr, respectively (Table 1). The mean $AUC_{0-\infty}$ of total radioactivity and unchanged CP-544439 was 635 µg-equiv of CP-544439-hr/mL and 102 µg-hr/mL. The mean terminal elimination half-life of total circulating radioactivity and unchanged CP-544439 was 13 and 3.8 hr, respectively.

Dog: After oral administration of 100 mg/kg of [^{14}C]CP-544439 to Beagle dogs, the mean C_{max} of total circulating radioactivity and unchanged CP-544439 was 30.2 µg-equiv of CP-544439/mL and 8.1 µg/mL, respectively, and the mean T_{max} was 1.25 and 0.75 hr, respectively (Table 1). The mean $AUC_{0-\infty}$ of total radioactivity and unchanged CP-544439 was 491 µg-equiv of CP-544439-hr/mL and 32.1 µg-hr/mL. The mean terminal elimination half-life of total circulating radioactivity and the unchanged CP-544439 was 40 and 3.4 hr, respectively.

DMD Fast Forward. Published on June 19, 2008 as DOI: 10.1124/dmd.108.022566
This article has not been copyedited and formatted. The final version may differ from this version.

Excretion

Rats: The recovery of the radiolabeled material was essentially complete after oral administration of a single 250 mg/kg dose of [^{14}C]CP-544439 to SD rats. About 63% of the dose was excreted in the feces while 37% of the dose was excreted in the urine after 168 hr, resulting in an overall recovery of 100% (Table 2). There were no gender differences in the excretion pattern of rats (data not shown). Most of the radioactivity was recovered in the initial 48 hr in all rats.

Dogs: The feces was the primary route of excretion in Beagle dogs after a single oral administration of [^{14}C]CP-544439 at a dose of 100 mg/kg. Table 2 shows the percentage of radioactivity excreted in the urine and feces over 168 hr post dose. A total 8.2 and 92.8 % of the administered dose was excreted in the urine and the feces of the male and female dogs over 168 hr respectively, resulting in a total recovery of approximately 100% (Table 2). As in rats most of the dose was recovered in the first 48 hr after dosing of the radiolabeled compound. No gender differences were observed in the excretion pattern of the compound in dogs as well.

Distribution

Plasma Protein Binding: CP-544439 is a weakly acidic compound with a *p*K_a of 8.7 and is hydrophilic with experimental Log P of 1.51. Plasma protein binding for CP-544439 in rat, dog and human plasma was determined by equilibrium dialysis method at concentrations of 500, 1000 and 2500 ng/mL. CP-544439 exhibited moderate plasma protein binding at values ranging from 88, 90 and 89% at 1 μg/mL in rat, dog and human. There was no change in the free fraction of CP-544439 at the concentrations of

0.5 and 2.5 μg/mL suggesting that the percentage of CP-544439 bound to plasma proteins was independent of its plasma concentrations in all species. The extent of protein binding of CP-544439 to human serum albumin (HSA) and alpha-1 glycoprotein (AAG) was also determined to assess the specificity of the compound towards the two common proteins found in plasma. The percentage of unbound CP-544439 was 16 and 93% in HSA and AAG solutions, respectively. This suggested that HSA was the major binding protein for CP-544439 in human plasma.

Incubation of CP-544439 with rat, dog and human plasma was also conducted to assess the hydrolysis of the compound by plasma esterases. This resulted in a half-life of ~52 min when CP-544439 was incubated with rat plasma. However, no turnover was observed when the compound was incubated with dog and human plasma resulting in a half-life of > 300 min in both species.

Tissue distribution: Tissue distribution of CP-544439 was investigated by WBAL following an oral 275 mg/kg dose of [^{14}C]CP-544439. [^{14}C]CP-544439 radioequivalents were absorbed and distributed into most tissues of Long-Evans female and male rats after a single oral bolus dose. Table 3 depicts [^{14}C]CP-544439 radioequivalents expressed as μg eq/g in tissues from female and male rats. The absorption and distribution was rapid since most tissues showed radioactivity levels by 1 hr after dosing in both genders. [^{14}C]CP-544439 radioequivalents achieved C_{max} at 6 hr in the female rat and at 18 hr in the male rat in most tissues with few exceptions (Table 4). One exception was the periodontal ligament which achieved C_{max} at 168 hr in both genders. All but 6 tissues in the male and female rats were devoid of radioactivity by 36 hr post dose suggesting that [^{14}C]CP-544439 radioequivalents were eliminated rapidly from the

body. The liver, lung, periodontal ligament, myocardial blood, kidney, and exorbital lacrimal gland sustained radioactivity equivalents for at least 36 hr. By 168 hr post dose the periodontal ligament was the only tissue containing [^{14}C]CP-544439 radioequivalents in both rat genders. The apparent $t_{1/2}$ for most female and male tissues could not be determined since a definitive elimination phase was not discernible. For the female rat, only four tissues (i.e. liver, myocardial blood, exorbital lacrimal gland and the kidney) had measurable $t_{1/2}$ that ranged from 8 to 22 hr. The apparent $t_{1/2}$ of [^{14}C]CP-544439 radioactivity in the whole-body was approximately 6 hr for both rat genders.

The highest concentrations of [^{14}C]CP-544439 radioequivalents were found in the GIT tract in both genders as was expected. Drug-associated radioactivity present in GIT contents plausibly represented unabsorbed [^{14}C]CP-544439 as well as [^{14}C]CP-544439 related material that was excreted via the bile or intestinal secretion. Interestingly the periodontal ligament showed high concentrations of radioequivalents even at 168 hr post dose resulting exposures of 8765 and 9921 μg eq·h/g in the female and male rat (Table 4). Assessment of the tissues in the central nervous system indicated that [^{14}C]CP-544439 radioequivalents primarily distributed into the cerebellum and cerebrum. All other CNS tissues did not show any appreciable levels of radioequivalents except at 1 h post dose (Table 3). Drug equivalents did not distribute into ocular tissues that lacked melanin since radiolabel was only detected in the uvea, a melanin containing tissue, up to 6 to 18 hr post dose. The exposure of [^{14}C]CP-544439 in the uvea of the female and male rat was 34 and 147 μg eq·hr/g, respectively (Table

4). The reason for the 4-fold higher exposure to radioactivity in the male rat is not known.

Some other gender differences were also observed in the distribution of [^{14}C]CP-544439. The male exorbital lacrimal gland depicted a 24-fold greater exposure to the radiolabel than the female rat whereas the male liver showed 1.8-fold greater radioequivalents. The whole-body exposure to [^{14}C]CP-544439 radioequivalents also was approximately 2-fold higher in the male rat than in the female.

Metabolism of CP-544439

The metabolism of CP-544439 in rat and dog was assessed by profiling urine, bile, plasma and the fecal homogenate from the two species. As a first step the biological matrices from the rat and dog were pooled to account for >95% of the radioactivity.

Rat: Representative HPLC-radiochromatograms of the extracted urinary (urine pooled from 0 –72 hr) and fecal (pooled from 0-48 hr) samples from rat are shown in Figure 2. The mean percentage of each metabolite excreted in rat urine and feces is shown in Table 5. The urinary profile showed 6 peaks including the unchanged CP-544439 (Figure 2A). Only 8.3% of the dose was excreted as unchanged CP-544439 (ret time 18.33 min) in the rat urine. Major peaks eluting at 21.3, 24.3, 16.7 and 14.3 min represented metabolites M2, M3, M5 and M6 and accounted for 6.6, 5.3, 6.0 and 4.3% of the dose, respectively, whereas peak eluting at 10.1 min represented metabolite M1 and constituted a mean 1.2% of the dose. Metabolite M4 was detected as a minor metabolite in the radiochromatogram and almost co-eluted with M2. Hence its relative abundance in the urinary profile could not be determined. The peak eluting at 1.5 min

was not identified and represented 2.2% of the dose. The HPLC-radiochromatogram of the fecal extract showed 5 peaks including unchanged CP-544439 (Figure 2B). The major radioactive peak was unchanged CP-544439 and accounted for 29% of the dose (Table 5). The peaks eluting at 21.3 and 24.3 min represented M2 and M3 and accounted for 19 and 3.9 % of the dose, respectively. Other peaks, M6 and M7 eluting at 16.7 and 7.4 min represented 4.6 and 2.2% of the dose respectively.

The radiochromatogram of the rat bile is shown in Figure 3A. Since bile was collected for 24 hr only, the abundance of metabolites was expressed as percentage of radioactivity. The major peak was M1 and eluted at ~10 min representing 75.8 % of the total radioactivity excreted in bile in 24 hr. Metabolite M3 eluted at 26.4 min and co-eluted with a M8 a new peak that was not observed in the urine or feces. The metabolites together represented 6.1% of the radioactivity. Metabolite M2 eluted at 23.2 min and accounted for 2.6% of the radioactivity. The unknown peaks eluting at 1.4 to 6.05 min accounted for 4.7% of the radioactivity.

Approximately 89% of the circulating radioactivity in the plasma pooled from 0 to 72 hr post dose could be identified. The rest could not be distinguished from the background. Three metabolites and unchanged CP-544439 were present in the plasma (Figure 3B). Metabolites M1, M2, M3 and the unchanged CP-544439 accounted for most of the radioactivity and constituted 2.9, 23, 32.8 and 10.7% of the circulating radioactivity, respectively (Figure 3B).

Dog: The analysis of pooled urine sample (0-72 hr) showed 7 peaks including the unchanged CP-544439 (Figure 4A) in HPLC-radiochromatogram. Unchanged CP-544,439 represented only 1.5 % of the dose excreted in the urine (Table 5). Metabolite

M1, eluting at 11 min was the major urinary metabolite representing 3.2% of the dose. Other peaks representing metabolites M2, M3 & M8, M5, M6 and M7 were also detected in the urine but each metabolite represented <1 % of the radioactive dose. All metabolites together accounted for 2.4 % of the excreted dose. The HPLC-radiochromatogram of the fecal extract pooled from 0-72 hr showed only one peak eluting at ~20 min accounted 100% of the dose excreted in the feces (Figure 4B, Table 5). Similarly, profiling of the bile sample from the collected from 0-8 hr from bile-cannulated dog showed only one peak eluting at 11 min and accounted for 100% of the radioactivity excreted in the bile (Figure 5A). The retention times of the peaks in the fecal extract was similar to that of the unchanged CP-544439 and the peak at 11 min in the bile represented metabolite M1.

Approximately 88% of the circulating radioactivity in the plasma pooled at 0-72 hr post dose could be identified (Figure 5B). The rest could not be distinguished from the background. Five major peaks and 3 minor metabolites were observed in the radiochromatogram of dog plasma that was constructed after collecting fractions and counting the radioactivity in each fraction. The retention times at 11, 19, 21.3 and 24.7 matched those of metabolites M1, CP-544439, M2 and a mixture of M3 and M8 and accounted for 24, 31, 4.0 and 8.7% of the total circulating radioactivity. In the mixture of M3 and M8 eluting at 24.7 min, M8 was the major constituent whereas M3 represented a minor metabolite. However, an exact abundance could not be determined from the data. A new peak eluting at 8.3 min (M9) was also observed in the plasma profile and accounted for 7.0% of the total circulating radioactivity (Figure 5B).

Metabolic Profiles of CP-544439 in Human Plasma and Urine

The plasma and urine obtained from healthy human volunteers dosed with CP-544439 at 1000 mg QD in a clinical pharmacology dose escalation study was analyzed to assess the metabolic profile of CP-544439 in humans in vivo. The high dose was selected for metabolite profiling to ensure that all metabolites were detected in the human plasma. Since the CP-544439 dosed to healthy human volunteers was unlabeled only a qualitative assessment of metabolites was possible. However, presence of the UV detector in line with the mass spectrometer gave an idea of major and minor metabolites that were circulating or excreted in humans. The UV chromatogram of plasma and urine showed 4 and 6 peaks respectively, the retention times of which were similar to M1 at 11 min, CP-544439 at 19 min, M2 at 22 min and M3 at 24.7 min in the rat and dog (Figure 6). The UV chromatogram of human urine showed 2 additional peaks eluting at 18 and 19 min respectively, which were similar to metabolites M5 and M6 observed in rat urine (Figure 6B).

Metabolite Identification

The structures of metabolites were elucidated by ionspray LC-MS/MS using a combination of full precursor ion and neutral loss scanning techniques. All metabolites were further characterized using the product ion scans of the identified masses. CP-544439 gave a good signal at m/z 409 in a full scan, in the negative ion mode. The parameters of the mass spectrometer were thus optimized in this mode for the product ions of *m/z* 409.

The proposed characteristic molecular ion $[M-H]^-$ and product ions of CP-544439 and its metabolites are depicted in Scheme 1. The product ion mass spectrum of m/z 409 gave one major characteristic fragment ion at *m/z* 266. This ion represented the sulfonamide

moiety of the molecule. Other minor fragment ion was observed at *m/z* 251 which suggested a loss of ammonia from *m/z* 266 as shown in Scheme 1. The precursor ion scan of *m/z* 266 was therefore used to identify metabolites that had modifications on the tetrahydropyranyl-hydroxamate moiety. Other LC/MS/MS experiments conducted were the precursor ion scan of *m/z* 282 which corresponded to the oxidized sulfonamide group (*m/z* 266 + 16). No attempt was made to isolate the metabolites to obtain conclusive NMR spectra however the structures of metabolites were confirmed by comparison of their retention time and mass spectra with the synthetic standards of the metabolites were available. The structures/proposed structures of metabolites of CP-544439 are shown in Scheme 2.

Metabolite M1 showed a signal at *m/z* 585 in the precursor ion scan of *m/z* 266 in negative ion mode. The molecular ion of *m/z* 585 suggested an addition of 176 amu to m/z 409. The product ion mass spectrum of *m/z* 585 showed fragment ions at *m/z* 409, 266, 251 and 193 (Scheme 1). The fragment ions at *m/z* 409, 266 and 251 were consistent with the molecular ion of CP-544439 and fragment ions observed in the mass spectrum of *m/z* 409 where as the ion at *m/z* 193 corresponded to the *O*-glucuronic acid moiety. This suggested that M1 was a glucuronide conjugate of CP-544439. This was further confirmed by treatment of the plasma or urine sample with β-glucuronidase which resulted in the generation of the parent compound.

Metabolite M2 gave a strong signal at *m/z* 393 in the precursor ion scan of *m/z* 266. The product ion mass spectrum of *m/z* 393 gave major fragment ions at *m/z* 350, 329, 266 and 251 in the negative ion mode (Scheme 1). The fragment ion at *m/z* 350 indicated a loss of 43 amu suggesting a loss of the amide moiety. The ion at *m/z* 329

(loss of 64 amu) indicated a loss of the SO_2 moiety. Recent reports have demonstrated that some pharmaceutical aromatic sulfonamides eliminate SO_2 upon CID in the positive or negative ion mode in API MS (Wang et. al., 2003). The ions at *m/z* 266 and 251 were similar to those observed in the parent and suggested that the sulfonamide moiety was intact. The retention time and the product ion mass spectrum of the metabolite were similar to the mass spectrum of the authentic standard of the amide (data not shown) further confirming that M2 was an amide analog of CP-544439.

Metabolite M3 gave a strong signal at *m/z* 394 in the precursor ion scan of *m/z* 266 The product ion mass spectrum of *m/z* 394 gave fragment ions at *m/z* 350, 266 and 251, in the negative ion mode (Scheme 1). The fragment ion at *m/z* 350 indicated a loss of the carboxy group (44 amu). The ions at *m/z* 266 and 251 were similar to those observed in the mass spectrum of M2 and CP-544439 and suggested that the sulfonamide moiety was intact as seen in M2. Comparison of the retention time and product ion mass spectrum of the metabolite with that of authentic standard of the carboxylic acid analog of CP-544439 indicated that the M3 was a carboxylic acid.

Metabolite M4 which co-eluted with M2 in the chromatogram of the rat urine gave a signal at *m/z* 407 in the precursor ion scan of m/z 266, respectively, suggesting an addition of 14 amu to *m/z* 393. The product ion mass spectra of *m/z* 407 gave fragment ions at *m/z* 335, 266 and 251 in the negative ion mode (Scheme 1). The presence of ions at *m/z* 266 and 251 suggested that the sulfonamide moiety was intact as observed previously and indicating that the tetrahydropyranyl moiety was modified possibly to a tetrahydropyrone. The ion at m/z 335 indicated a loss of 72 amu and suggested a

cleavage of the tetrahydropyrone moiety. Based on this data the metabolites were proposed to be lactone of the amide.

Metabolites M5 and M6 gave strong signals at *m/z* 409, a ion similar to CP-544439, in the precursor ion scan of *m/z* 266. A molecular ion similar to CP-544439 but a different retention time and modification of the sulfonamide containing moiety suggested that this metabolite resulted from the oxidation of the amide (M2). The product ion mass spectra of these two metabolites were similar and showed major fragment ions at *m/z* 335 and 266 (Scheme 1). The presence of an ion at *m/z* 266 confirmed that the sulfonamide moiety was intact. The ion at *m/z* 335 suggested a loss of 74 amu that probably resulted from the cleavage of the tetrahydropyrone moiety as observed in the fragmentation of M4. Based on this data, M5 and M6 were proposed as hydroxylated metabolites of the amide, M2. This was confirmed by incubation of synthetic M2 with rat liver microsomes in the presence of NADPH (data not shown). The detection of these two metabolites in the incubation mixture not only confirmed that M5 and M6 were oxidized metabolites of M2 but also showed that the amide was a substrate of P450. The metabolites were absent in the control (without NADPH) incubations. No attempt was made to further characterize the P450 involved in the oxidation of M2.

Metabolite M7 also showed a molecular ion at *m/z* 409 in the precursor ion scan of *m/z* 282. The absence of the signal in the precursor ion scan of m/z 266 indicated that the sulfonamide ring in this metabolite was modified. A molecular ion similar to CP-544439 but a different retention time and modification of the sulfonamide containing moiety suggested that this metabolite also resulted from the oxidation of the amide (M2). The product ion mass spectrum of M7 at *m/z* 409 resulted in the fragment ions at m/z 345,

282 and 267 (Scheme 1). All fragment ions observed in the mass spectrum of M7 were consistent with an addition of 16 amu to the fragment ions observed in the mass spectrum of M2. This data suggested that the amide underwent hydroxylation on one of the aromatic rings. However, the exact position of the hydroxyl group could not be ascertained from this data.

Metabolite M8 co-eluted with the acid, M3 and gave a strong signal at *m/z* 266 in the total ion scan. This indicated that the metabolite had lost its tetrahydropyranyl moiety and was a cleaved product of CP-544439. The product ion mass spectrum of *m/z* 266 gave a major fragment ion at *m/z* 202 and 107 (Figure 7A). The fragment ion at *m/z* 202 resulted from the rearrangement product following a loss of the SO_2 moiety from M8 as shown in Figure 7A. A loss of 64 amu was also observed in the fragmentation of the amide metabolite M2 (described above) and was characterisitic of the presence of the sulfonamide group in the molecule. The ion at *m/z* 107 probably resulted from further loss of the fluorophenyl moiety *m/z* 202. The mass spectral data suggested that the M8 was a sulfonamide metabolite of CP-544439. The retention time and the product ion mass spectrum of M8 was similar to that of the authentic sulfonamide standard and hence further confirmed its identity.

Metabolite M9 gave a signal at *m/z* 267 in the total ion scan. The product ion mass spectrum of *m/z* 267 gave major fragment ions at *m/z* 203, 172 and 108 (Figure 7B). The ion at *m/z* 172 indicated a loss of the fluorophenyl moiety from the molecule. The minor fragment ion at *m/z* 203 resulted from a loss of SO_2 moiety as was observed in M8 and M2 and the fragment ion at *m/z* 108 was a resulte of further cleavage and loss of the fluorophenyl moiety from *m/z* 203. Based on this data the metabolite was

proposed to be a sulfonic acid. No attempt was made to confirm the structure of the metabolite.

In Vitro Studies on Glucuronidation of CP-544439

Preliminary experiments were conducted to identify the primary UDP glucuronyltransferase (UGT) isoforms responsible for the glucuronidation of CP-544439 using 12 heterologously expressed human UGT (*Supersomes*). Figure 8 shows the amount of glucuronide conjugate formed following incubation of CP-544439 by various isoforms of UGT. All UGTs glucuronidated CP-544439 however, UGTs 1A3, 1A1 and 1A9 were the primary isoforms that catalyzed the formation of M1. No attempt was made to determine the K_m and V_{max} for this glucuronidation reaction.

DMD Fast Forward. Published on June 19, 2008 as DOI: 10.1124/dmd.108.022566
This article has not been copyedited and formatted. The final version may differ from this version.

Discussion

This study described the disposition and metabolism of [^{14}C]CP-544439 in rat and dog, the animal species used in safety toxicology studies, after oral administration. In addition, the circulating and urinary metabolic profile of CP-544439 in humans was assessed using the plasma and urine samples from the dose escalation study in healthy human volunteers to ensure that the selected animal species were exposed to all major metabolites formed in humans.

The radioactive dose was quantitatively recovered from urine and feces of both the rat and dog over a period of 168 hr. The recovery was essentially complete within 48 hr suggesting rapid excretion of CP-544439 and its metabolites. Most of the radioactivity was excreted in the feces of both species and probably consisted of unabsorbed dose and the dose that was excreted via the bile. No gender-related differences were observed in the two species. A proper assessment of total absorption could not be made in this study since bile was collected for a limited time for sake of profiling biliary metabolites.

Pharmacokinetic analysis of [^{14}C]CP-544439 and unchanged CP-544439 indicated that the exposure ($AUC_{0-\infty}$) of unchanged CP-544439 in rat and dog was 16 and 6.5% of the total radioequivalents, respectively, indicating that majority of the circulating radioactivity comprised of metabolites. In rat, the T_{max} of total radioactivity (8 hr) was longer than the T_{max} of unchanged CP-544439 (2.2 hr) suggesting that although the absorption of [^{14}C]CP-544439 was rapid, one or more metabolites of CP-544439 peaked at a later time. In contrast, the T_{max} of total radiolabel and unchanged CP-544439 in the dog was

1.25 and 0.75 hr, respectively, which suggested that one or more metabolites peaked at the same time as unchanged CP-544439. Only 26% of C_{max} constituted unchanged CP-544439 in dogs suggesting that the metabolites accounted most of the radioactivity in the peak concentrations. The terminal elimination half-life of the total radioactivity was longer than that of unchanged CP-544439 in both species signifying that some circulating metabolites had a longer half-life than CP-544439.

[^{14}C]CP-544439 distributed into most tissues of female and male Long-Evans rats except the central nervous system. Exposure to [^{14}C]CP-544439 in the cerebellum and cerebrum were similar to that of arterial blood. Poor distribution in the CNS illustrated minimal permeability of CP-544439 and its metabolites across the blood brain barrier. The uvea, a melanin containing tissue in the eye, also had minimal exposure to [^{14}C]CP-544439. Most radioactivity was eliminated from the uveal tract illustrating that this compound did not have a high affinity for melanin. The highest concentrations of radioequivalents were found in the contents of the GIT and probably resulted from unabsorbed material following oral administration or from biliary elimination of radioequivalents. The periodontal ligament showed maximum exposure to CP-544439 radioequivalents. The periodontal ligament is a group of specialized connective tissue fibers that essentially attaches a tooth to the alveolar bone within which it sits. These fibers are composed primarily of type I collagen and is highly vascularized. The persistent radioactivity associated with the periodontal ligament was probably due to the intense vascularization and collagen content of this structure. The lack of detectable radiolabel in other target tissues of interest (articulations of the skeletal system and macular region of the retina) was not surprising since the rats used in this study were

not affected with the neogenic vascularization associated with RA and age-related exudative macular degeneration. However, the marrow of the long and compact bone another target tissue of interest, demonstrated radioactivity up to 18 hr post dose.

CP-544439 was extensively metabolized in both species. Only 8.4 and 1.5% of the total dose constituted unchanged CP-544439 in the rat and dog urine, respectively, and there was no unchanged CP-544439 in the bile of the two species. Reduction of CP-544439 to M2 (Scheme 2) was the major route of metabolism in rats. It was a major component of the rat excreta (25.6% of the total dose) and accounted for 23% of the total circulating radioactivity. Further, some secondary oxidative metabolism M5, M6 and M7 were detected suggesting that the amide was a substrate for P450. Reduction of hydroxamates to amide has been previously reported and is catalyzed by aldehyde oxidase, a member of molybdenum cofactor-containing enzymes (Sugihara and Tatsumi, 1986; Sugihara et. al., 1983a, 1983b). Earlier work by Obach has demonstrated that aldehyde oxidase catalyzes conversion of CP-544439 to M2 (Obach, 2004). In contrast to rats, reduction of CP-544439 was a relatively minor pathway in dogs. This difference in the rat and dog was most likely related to the low activity of dog liver aldehyde oxidase (Kitamura, et. al., 1999; Beedham et. al. 1987; Acheampong, et. al. 1996).

Hydrolysis of CP-544439 to M3 (Scheme 2) was the second major pathway of metabolism of CP-544439 in the rat. It accounted for 9.2% of the total dose in the excreta and represented ~33% of the total circulating radioactivity. No downstream metabolites of M3 such as the acylglucuronide or any oxidative metabolites were detected in the urine or plasma. Unlike rat, M3 was also a minor metabolite in dogs.

Although the exact percent of circulating M3 could not be determined due to its co-elution with M8, the comparison of the peak areas of M3 in the extracted ion chromatogram of pooled plasma indicated that it was a minor circulating metabolite. The above result correlated with the in vitro studies with CP-544439 which showed instability of the compound in rat plasma but not in the dogs or humans. This was also consistent with reports which demonstrate that rat plasma has greater hydrolytic capability than other species (Allan et. al., 2006; Honohan et, al., 1980). Although it is possible that M3 was a result of the amidase catalyzed hydrolysis of the amide M2, incubation of synthetic M2 with rat plasma did not yield the corresponding M3. Furthermore, M2 was stable to chemical hydrolysis in buffer at acidic and basic pH ruling out the possibility of an artifact of a chemical hydrolysis in the mobile phase. This was consistent with earlier reports that have demonstrated the hydrolytic cleavage of hydroxamates to the corresponding carboxylic acid (Conejo-Garcia A, and Schofield CJ, 2005; Kobashi et. al., 1973)

CP-544439 was also converted to the glucuronide M1 in the rat and dog. It was the primary circulating metabolite in dog plasma (24% of the total radioactivity) and was the only metabolite detected in dog bile. In contrast the glucuronide conjugate M1 was only observed in rat bile and constituted 76% of biliary radioactivity. In addition, two novel metabolites resulting from cleavage of CP-544439 were also detected in the dogs. The sulfonamide metabolite (M8), which co-eluted with M3 and its hydrolytic product, the sulfonic acid metabolite M9, was primarily detected as a circulating metabolite. The mechanism for formation of M8 and M9 is unknown. However one plausible pathway could involve the Lossen rearrangement. This is a base catalyzed rearrangement of O-

acylhydroxamic acids that yield the corresponding isocyanates (Bauer and Exner 1974) which could then be converted to carbamates via treatment with appropriate alcohols or to amine via hydrolysis. A similar rearrangement of the conjugated CP-544439 can result in the formation of the isocyanate which can yield the corresponding M8 via hydrolysis and subsequent decarboxylation (Scheme 3). The sulfonic acid M9 is possibly a hydrolysis product of M8. It should be noted that such a rearrangement is unprecedented in biological systems to our knowledge. Also, the formation of O-acyl derivatives of hydroxamic acids such as the sulfate conjugate or the acetyl conjugates were not observed in the biological matrices of animal species.

Profiling of human plasma and urine revealed that metabolites of CP-544439 observed in the humans were similar to those observed in the rat and dog. Athough proper assessment of the amount of each circulating and urinary metabolite could not be made, the glucuronide conjugate was the major circulating and urinary metabolite in humans (based on the UV chromatogram). Preliminary experiments using heterologously expressed UGTs suggested that glucuronidation of CP-544439 was catalyzed predominantly by UGT1A1, UGT1A3 and UGT1A9. Determination of the kinetic parameters of glucuronidation by these three UGT isoforms was not attempted given the lack of the authentic glucuronide conjugate. UGT 1A1 is an enzyme that displays significant genetic polymorphism (Fisher et. al. 2001). Although metabolism by UGT1A1 that can lead to interindividual variability in exposure of CP-544439, such impact is not anticipated since CP-544439 is metabolized by several pathways in humans. Furthermore no safety concerns around the N-Oglucuronide (M1) are

anticipated given that these glucuronides do not undergo acylmigration unlike the acylglucuronides and no hydrolytic cleavage of these metabolites was observed.

In summary, CP-544439 is widely distributed to all tissues and is primarily eliminated via the feces. Biotransformation of CP-544439 occurs mainly via glucuronidation, reduction and hydrolysis of the hydroxamate moiety. All three pathways observed in humans are also prevalent in the rat and dog. Reduction of CP-544439 appears to be the primary route of metabolism in the rat whereas glucuronidation is the primary route of metabolism of CP-544439 in the dog and humans. Preliminary in vitro phenotyping studies suggest that glucuronide conjugate formation is primarily catalyzed by UGT1A1, UGT1A3 and UGT1A9 in humans.

DMD Fast Forward. Published on June 19, 2008 as DOI: 10.1124/dmd.108.022566
This article has not been copyedited and formatted. The final version may differ from this version.

Acknowledgement

We thank Vitrax, Placentia, CA for synthesizing [^{14}C]CP-544439 and the radiochemistry group at Pfizer Global Research in Groton for purifying the material. We also thank Primedica Corporation, Worcester, MA for conducting the animal studies.

References

Acheampong AA, Chien D-S, Lam S, Vekich S, Breau A, Usansky J, Harcourt D, Munk SA, Nguyen H, Garst M, Tang Liu, D (1996) Characterization of brimonidine metabolism with rat, rabbit, dog, monkey and human liver fractions and rabbit liver aldehyde oxidase. *Xenobiotica* **26**: 1035-1055.

Allan GA, Gedge JI, Nedderman ANR, Roffey SJ, Small HF, and Webster R (2006) Pharmacokinetics and metabolism of UK-383367 in rats and dogs: A rationale for long-lived plasma radioactivity. *Xenobiotica* **36**: 399-418.

Baillie TA, Cayen MN, Fouda H, Gerson RJ, Green JD, Grossman SJ, Klunk LJ, Leblanc B, Perkins DG, and Shipley LA (2002) Drug metabolites in safety testing. *Toxicol. Appl. Pharmacol.* **182**: 188-196.

Bauer L, and Exner O (1974) The Chemistry of Hydroxamic Acids and N-Hydroxyimides. *Angew. Chem. Int. Ed. Engl*. **13**: 376-384.

Beckett RP, Davidson AH, Drummond AH, Huxley P, and WhittakerMU. (1996) Recent advances in matrix metalloproteinase inhibitor research. *Drug Discovery Today* **1**: 16-26.

Beedham C, Bruce SE, Critchley DJ, Al-Tayib Y, Rance DJ (1987) Species variation in hepatic aldehyde oxidase activity. *Eur. J. Drug Metab. Pharmacokinet*. **12**: 307-310.

Conejo-Garcia A, and Schofield CJ (2005) A prodrug system for hydroxylamines based on esterase catalysis *Bioorg. Med. Chem. Lett*. **15**: 4004–4009.

Fisher MB, Paine MF, Strelevitz TJ, Wrighton SA. (2001) The role of hepatic and extrahepatic UDP-glucuronyltransferases in human drug metabolism. *Drug Metab. Rev.* **33**:273-297.

Hastings KL, El-Hage J, Jacobs A, Leighton J, Morse D, Osterberg R (2003) Drug metabolites in safety testing. *Toxicol. Appl. Pharmacol.* **190**: 91-92.

Honohan T, Fitzpatrick FA, Booth DG, McGrath JP, Morton DR, and Nishizawa EE (1980) Hydrolysis of an orally active platelet inhibitory prostanoid amide in the plasma of several species. *Prostaglandins* **19**: 123-138.

Kitamura S, Sugihara K, Nakatani K, Ohta S, Oh-hara, T, Ninomiya, S, Green, CE, Tyson, CA (1999) Variation of hepatic methotrexate 7-hydroxylase activity in animals and humans *IUBMB Life* **48**: 607-611.

Kobashi K, Takebe S, and Hase J (1973) Distribution, metabolism and excretion of caprylo- and nicotinohydroxamic acid. *Yakugaku Zasshi* **93**: 1564-1572.

Michaelides MR, and Curtin ML. (1999) Recent advances in matrix metalloproteinase inhibitors research. *Curr. Pharm. Design* 5: 787-819.

Obach RS (2004) Potent inhibition of human liver aldehyde oxidase by raloxifene. *Drug Metab. Dispos.* **32**: 89-97.

Otterness IG, Bliven ML, Eskra JD, tsKopple JM, Stukenbrok HA, and Milici AJ (2000) Cartilage damage after intraarticular exposure to collagenase 3. *Osteoarthritis Cartilage* **8**: 366-373.

Potchoiba MJ, Tensfeldt TG, Nocerini MR and Silber BM (1995) A novel quantitative method for determining the biodistribution of radiolabeled xenobiotics using whole-body cryosectioning and autoradioluminography. *J. Pharmacol. Exp. Ther.* **272**: 953-962.

Potchoiba MJ, West M, and Nocerini MR (1998) Quantitative comparison of autoradioluminography and radiometric tissue distribution studies using carbon-14 labeled xenobiotics. *Drug Metab. Disp.* **26**: 272-277.

Prakash C and Soliman V (1997) Metabolism and excretion of a new anxiolytic drug candidate, CP-93393, in Long-Evans rats. *Drug Metab. Dispos* **25**: 1288-1297.

Rao BG (2005) Recent developments in the design of specific matrix metalloproteinase inhibitors aided by structural and computational studies. *Cur*. *Pharm*. *Design* **11**: 295-322.

Reiter LA, Robinson RP, McClure KF, Jones CS, Reese MR, Mitchell PG, Otterness IG, Bliven ML, Liras J, Cortina SR, Donahue KM, Eskra JD, Griffiths RJ, Lame ME, Lopez-Anaya A, Martinelli GJ, McGahee SM, Yocum SA, Lopresti-Morrow LL, Tobiassen LM, and Vaughn-Bowser ML (2004) Pyran-containing sulfonamide hydroxamic acids: potent MMP inhibitors that spare MMP-1. *Bioorg. Med. Chem. Lett*. **14**: 3389-3395.

Sugihara K Kitamura S and Tatsumi K (1983b) Involvement of liver aldehyde oxidase in conversion of N-hydroxyurethane to urethane. *J. Pharmacobio-dynamics* **6**: 677-683.

Sugihara K, and Tatsumi K (1986) Participation of liver aldehyde oxidase in reductive metabolism of hydroxamic acids to amides. *Arch. Biochem. Biophysics* **247**: 289-293.

Sugihara K, Kitamura S; and Tatsumi, K (1983a) Evidence for reduction of hydroxamic acids to the corresponding amides by liver aldehyde oxidase. *Chem. Pharm. Bull*. **31**: 3366-3369.

Ullberg S (1977) The technique of whole-body autoradiography cryosectioning of large species specimens. *Sci. Tools (Special Edition)* 1-32.

Wang Z, Hop CECA, Kim MS, Huskey SEW, Baillie TA, Guan Z. The unanticipated loss of SO2 from sulfonamides in collision-induced dissociation. *Rapid Commun. in Mass Spectrometry* 2003; 17: 81.

Figure Legends

Figure 1. Mean plasma concentration-time profile curves of CP-544439 and total radioactivity in SD rats and Beagle dogs after oral administration of [^{14}C]CP-544439.

Figure 2. HPLC-radiochromatograms of CP-544439 metabolites in urine (0-72 hr) and feces (0-48 hr) of SD rats after single oral dose of [^{14}C]CP-544439.

Figure 3. HPLC-radiochromatograms of CP-544439 metabolites in A) rat bile (0-24 hr) and B) rat plasma (0-72 hr) after single oral dose of [^{14}C]CP-544439.

Figure 4. HPLC-radiochromatograms of CP-544439 metabolites in urine (0-72 hr) and feces (0-48 hr) of Beagle dog after single oral dose of [^{14}C]CP-544439.

Figure 5. HPLC-radiochromatograms of CP-544439 metabolites in A) bile (0-8 hr) and B) plasma (0-72 hr) of Beagle dogs after single oral dose of [^{14}C]CP-544439.

Figure 6. HPLC-UV chromatograms of CP-544439 metabolites in A) pooled human plasma and B) pooled human urine after administration of 1000 mg dose of CP-544439 (QD) obtained from a dose escalation clinical pharmacology in human volunteers.

Figure 7. Product ion mass spectrum of metabolites A) M8 and B) M9 at *m/z* 266 and 267 in a negative ion mode.

Figure 8. Percentage of glucuronide conjugate (M1) formed following incubation of CP-544439 (20 μM) with heterolgously expressed UGT isoforms (Supersomes).

DMD Fast Forward. Published on June 19, 2008 as DOI: 10.1124/dmd.108.022566
This article has not been copyedited and formatted. The final version may differ from this version.

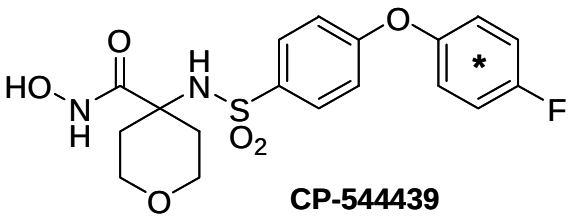

CP-544439

Asterisk indicates the site of radioactivity

Chart 1. Structure of CP-544439 4-[4-(4-Fluorophenoxy)-benzenesulfonylamino]tetrahydropyran-4-carboxylic acid hydroxyamide.

DMD Fast Forward. Published on June 19, 2008 as DOI: 10.1124/dmd.108.022566
This article has not been copyedited and formatted. The final version may differ from this version.

Scheme 1. Major collision induced dissociation product ions of CP-544439 and its metabolites.

Metabolites		[M-H]$^-$	Fragment Ions			
CP-544439	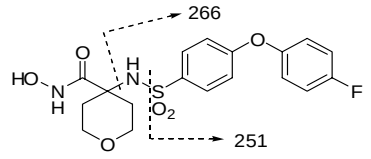	409	266	251		
M1	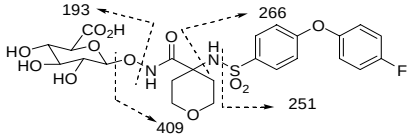	585	409	266	251	193
M2	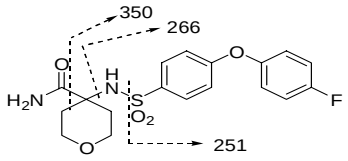	393	350	266	251	329
M3	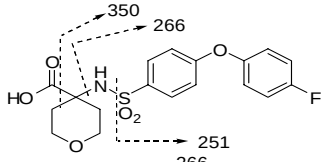	394	350	266	251	
M4	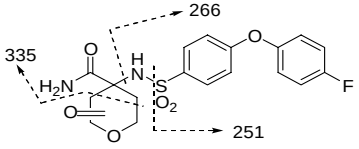	407	335	266	251	
M5	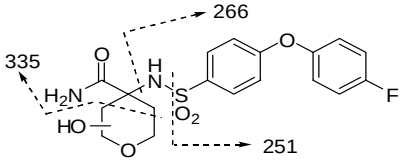	409	335	266	251	
M6		409	335	266	251	
M7	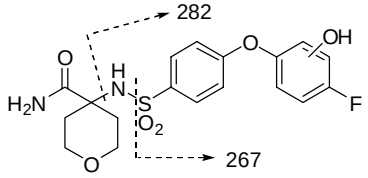	409	345	282	267	
M8	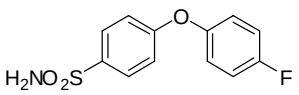	266	See Figure 7A			
M9	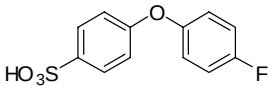	267	See Figure 7B			

DMD Fast Forward. Published on June 19, 2008 as DOI: 10.1124/dmd.108.022566
This article has not been copyedited and formatted. The final version may differ from this version.

Scheme 2. Proposed metabolic scheme of CP-544439 in SD rats, Beagle dogs and humans.

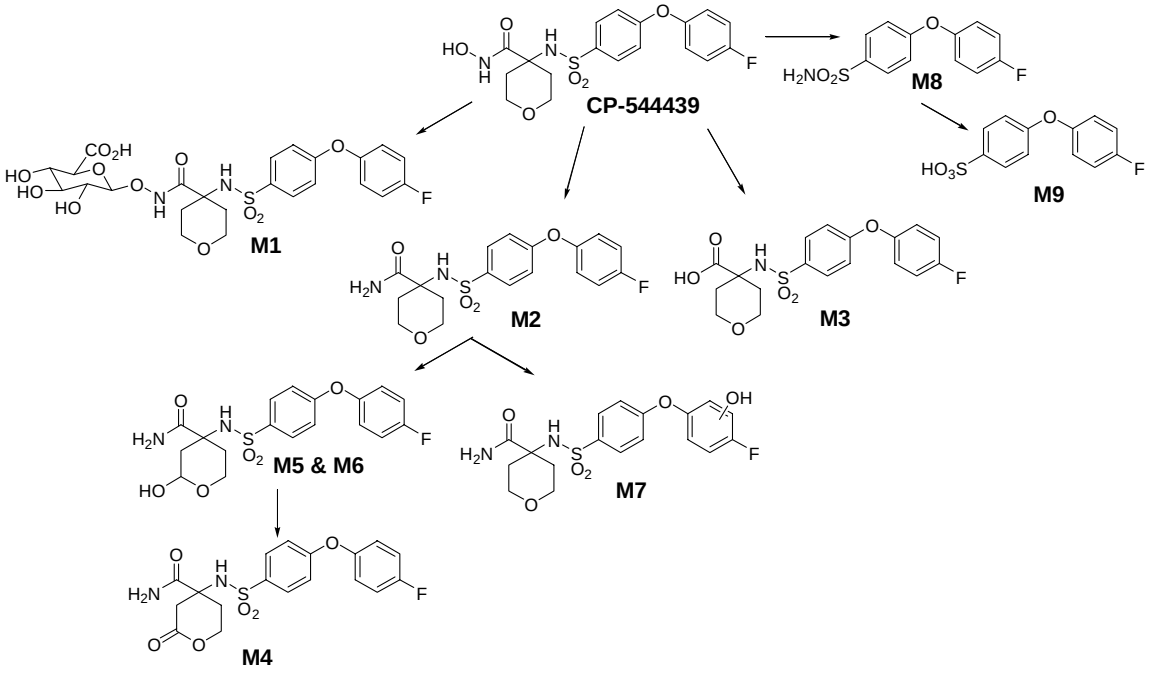

DMD Fast Forward. Published on June 19, 2008 as DOI: 10.1124/dmd.108.022566
This article has not been copyedited and formatted. The final version may differ from this version.

Scheme 3. Proposed mechanism for the formation of metabolites M8 and M9.

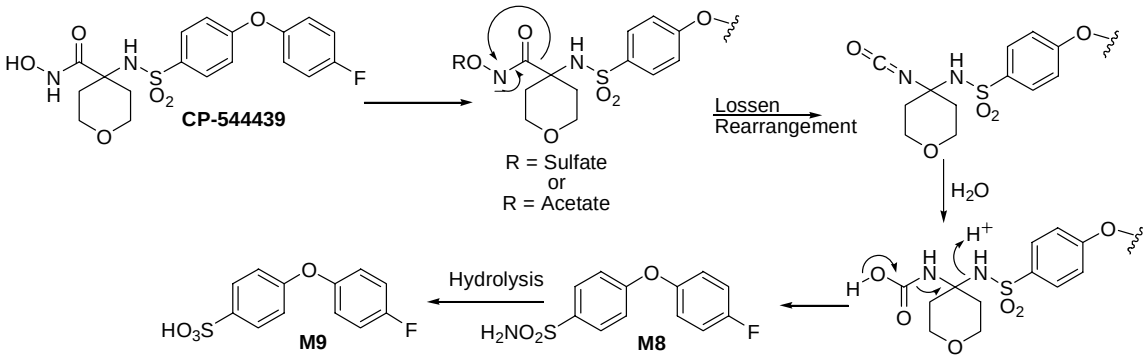

Table 1. Mean pharmacokinetic parameters of CP-544439 and total radioactivity in rats and dogs following oral administration of [^{14}C]CP-544439.

	Species	**N**	**T_{max}** *hr*	**C_{max}** *ug/ml*	**$AUC_{(0\text{-}tlast)}$** *ug-hr/mL*	**$AUC_{(0\text{-}\infty)}$**[a] *ug-hr/mL*	**$t_{1/2}$** *hr*
Total Radioactivity	Rat	6	8.0±3.1	24.0+5.54	621±101	635±106	13±1.0
Unchanged CP-544439	Rat	6	2.2±1.0	12.7+2.67	95.5±40.8	102±36.6	3.8±2.5
Total Radioactivity	Dog	4	1.25±0.50	30.2+5.25	338±151	491±301	40±30
Unchanged CP-544439	Dog	4	0.75±0.29	8.08+0.81	31.0±7.72	32.1±7.97	3.5±1.3

a) C_{max} and AUC values for total radioactivity are expressed as μg equiv/mL and μg equiv-hr/mL, respectively.

Table 2. Mean percentage of dose excreted in urine and feces from rats and dogs following oral administration of [^{14}C]CP-544439.

Time	Urine	Feces	Total
	Rats		
0-24	29	52	81
24-48	5.5	8.5	14
48-72	1.2	1.3	2.5
72-96	0.6	0.35	0.95
96-120	0.37	0.6	0.97
120-144	0.21	0.29	0.5
144-168	0.12	0.07	0.19
0-168	**37**	**63**	**100**
	Dogs		
0-24	5.0	56	61.0
24-48	1.7	34	35.7
48-72	0.68	2.1	2.8
72-96	0.31	0.4	0.7
96-120	0.2	0.14	0.3
120-144	0.18	0.08	0.3
144-168	0.15	0.09	0.2
0-168	**8.2**	**92.8**	**101**

DMD Fast Forward. Published on June 19, 2008 as DOI: 10.1124/dmd.108.022566
This article has not been copyedited and formatted. The final version may differ from this version.

Table 3. Tissue concentrations[a] of drug radioequivalents (μg eq/g) in female and male Long-Evans rats administered an oral dose (275 mg/kg) of [^{14}C]CP-544439.

	Female Rats						Male rats					
	1 h	3 h	6 h	18 h	36 h	168 h	1 h	3 h	6 h	18 h	36 h	168 h
Adipose: Brown	10	5	20	4	-----[b]	-----	6	8	11	18	-----	-----
Adrenal Gland	17	9	24	6	-----	-----	9	11	17	26	-----	-----
Blood: Arterial	16	11	24	-----	-----	-----	14	17	20	-----	-----	-----
Blood: Hepatic	14	9	14	-----	-----	-----	13	13	21	22	-----	-----
Blood: Myocardial	17	9	22	13	4	-----	12	17	20	22	5	-----
Blood: Venous	16	9	19	11	-----	-----	12	14	18	23	-----	-----
Bone Marrow: Femur	-----	6	18	8	-----	-----	11	12	12	17	-----	-----
Bone Marrow: Vertebra	8	4	12	8	-----	-----	6	11	9	9	-----	-----
Buccal Gland	-----	-----	15	-----	-----	-----	-----	6	7	14	-----	-----
Cerebellum	4	-----	6	4	-----	-----	-----	5	5	11	-----	-----
Cerebrum	4	-----	7	4	-----	-----	-----	6	5	10	-----	-----
Clitoridean\Preputial Gland	5	4	17	8	-----	-----	7	8	8	31	-----	-----
Gastric Mucosa	13	19	22	7	-----	-----	25	20	12	15	-----	-----
Harderian Gland	-----	-----	21	-----	-----	-----	5	22	41	43	-----	-----
Kidney	29	16	46	9	4	-----	20	25	27	34	-----	-----
Lacrimal Gland: Exorbital	8	4	-----	4	-----	-----	7	48	60	81	3	-----
Lacrimal Gland: Intraorbital	13	4	19	5	-----	-----	6	19	15	27	-----	-----
Lens	-----	-----	-----	-----	-----	-----	-----	-----	-----	4	-----	-----
Liver	45	21	47	11	5	-----	34	44	42	46	5	-----
Lung	14	8	19	10	-----	-----	10	14	17	21	4	-----
Muscle	5	-----	10	-----	-----	-----	3	4	6	9	-----	-----
Myocardium	11	6	19	6	-----	-----	8	12	15	19	-----	-----
Pancreas	8	7	22	3	-----	-----	7	9	13	18	-----	-----
Parotid Gland	7	4	19	-----	-----	-----	5	7	12	19	-----	-----
Peridontal Ligament	12	4	34	50	33	80	7	9	11	26	38	99
Renal Cortex	20	13	35	-----	-----	-----	14	20	21	28	-----	-----
Renal Medulla	39	19	53	-----	-----	-----	24	29	30	41	-----	-----
Salivary, Sublingual	11	5	11	-----	-----	-----	7	11	-----	20	-----	-----
Salivary, Submaxillary	9	5	19	5	-----	-----	6	10	13	20	-----	-----

DMD Fast Forward. Published on June 19, 2008 as DOI: 10.1124/dmd.108.022566
This article has not been copyedited and formatted. The final version may differ from this version.

Seminal Vesicle	NP[c]						10	23	13	42	-----	-----
Skin	4	-----	6	5	-----	-----	3	4	4	7	-----	-----
Spleen	9	3	15	5	-----	-----	8	10	10	13	-----	-----
Ovary\Testis	8	-----	13	5	-----	-----	-----	-----	-----	-----	-----	-----
Thymus	4	-----	8	-----	-----	-----	-----	5	6	0	-----	-----
Uvea	5	3	12	-----	-----	-----	5	6	6	13	-----	-----
Whole-Body	31	80	104	11	4	-----	42	143	146	58	3	-----
Gastro-intestinal Contents												
Cecum	542	663	1513	110	34	-----	95	236	1722	709	12	-----
Colon	1475	394	1852	197	-----	-----	736	3784	3254	632	21	-----
Gastric	>ULOQ[d]	3864	556	4	-----	-----	3494	1305	14	107	-----	-----
Intestine	799	436	608	60	24	-----	603	883	578	393	24	-----
Rectum	-----	-----	6427	217	26	-----	-----	354	3474	713	27	-----

[a] Mean radioequivalent concentrations (µg eqiv./g) were calculated by averaging tissue concentrations measured at different sectioning levels and/or from replicate cryosections obtained from the same sectioning level.

[b] Drug radioequivalents were not determined (-----) because the tissue radioactivity declined below the LLOQ (3.3 nCi/g), tissue not sampled, or the tissue was indistinguishable from background.

[c] Tissue not present in this gender.

[d] The upper limit of quantitation (ULOQ) was 21,475 nCi/g.

DMD Fast Forward. Published on June 19, 2008 as DOI: 10.1124/dmd.108.022566
This article has not been copyedited and formatted. The final version may differ from this version.

Table 4. Tissue pharmacokinetic parameters[a] of drug radioequivalents in female and male rats following oral administration of [^{14}C]CP-544439 at a dose of 275 mg/kg.

	Female Rat				Male Rat			
	$AUC_{0\text{-}Tlast}$	C_{max}	T_{max}	$t_{1/2}$	$AUC_{0\text{-}Tlast}$	C_{max}	T_{max}	$t_{1/2}$
Adipose: Brown	204	20	6	-----[b]	221	18	18	-----
Adrenal Gland	257	24	6	-----	329	26	18	-----
Blood: Arterial	89	25	6	-----	94	20	6	-----
Blood:Hepatic	65	15	1	-----	339	22	18	-----
Blood: Myocardial	436	22	6	11	579	22	18	-----
Blood: Venous	256	19	6	-----	328	23	18	-----
Bone Marrow: Femur	198	18	6	-----	240	17	18	-----
Bone Marrow: Vertebra	156	12	6	-----	160	11	3	-----
Buccal Gland	-----	15	6	-----	155	14	18	-----
Cerebellum	87	6	6	-----	119	12	18	-----
Cerebrum	95	7	6	-----	117	10	18	-----
Clitoridean\Preputial Gland	196	17	6	-----	275	31	18	-----
Gastric Mucosa	270	22	6	-----	270	25	1	-----
Harderian Gland	-----	21	6	-----	625	43	18	-----
Kidney	601	46	6	8	505	35	18	-----
Lacrimal Gland: Exorbital	77	7	1	22	1828	81	18	-----
Lacrimal Gland: Intraorbital	206	19	6	-----	325	26	18	-----
Liver	680	47	6	9	1218	46	18	-----
Lung	242	19	6	-----	520	21	18	-----
Muscle	39	10	6	-----	112	9	18	-----
Myocardium	207	19	6	-----	267	18	18	-----
Ovary	165	8	1	-----	NP[c]			
Pancreas	216	22	6	-----	245	18	18	-----
Parotid Gland	51	19	6	-----	228	19	18	-----
Peridontal Ligament	8765	80	168	-----	9921	99	168	-----
Renal Cortex	114	35	6	-----	396	28	18	-----
Renal Medulla	185	53	6	-----	579	41	18	-----

Salivary Gland: Sublingual	44	11	1	-----	252	20	18	-----
Salivary Gland: Submaxillary	201	19	6	-----	250	20	18	-----
Seminal Vesicle	NP				420	42	18	-----
Skin	90	5	6	-----	92	7	18	-----
Spleen	171	15	6	-----	182	13	18	-----
Thymus	34	8	6	-----	22	5	6	-----
Uvea	34	12	6	-----	147	13	18	-----
Whole-Body	1220	104	6	6	2416	145	6	6

[a] $AUC_{(0\text{-}Tlast)}$ values (µg eq·h/g) were calculated using linear trapezodial approximation. $T_{1/2}$ (h) was calculated as $0.693/K_{el}$. C_{max} and T_{max} values were reported as µg eq/g and h, respectively.

[b] The $t_{1/2}$ and $AUC_{0\text{-}tlast}$ were not determined (-----) because a definitive elimination phase was not discernable.

[c] Tissue not present in this gender.

DMD Fast Forward. Published on June 19, 2008 as DOI: 10.1124/dmd.108.022566
This article has not been copyedited and formatted. The final version may differ from this version.

Table 5. Mean percentage of the dose of urinary and fecal metabolites of CP-544439 in SD rats and Beagle dogs following oral administration of [^{14}C]CP-544439.

Metabolite	Percentage of Dose					
	Rat			Dog		
	Urine	Feces	Total	Urine	Feces	Total
CP-544439	8.3	29	37.3	1.5	95	96.5
M1	1.2	ND	1.2	3.2	ND	3.2
M2	6.6	19	25.6	0.48	ND	0.48
M3	5.3	3.9	9.2	0.67	ND	0.67
M4[1]	*Co-eluted with M2*			ND	ND	ND
M5	6.0	ND	6.0	0.43	ND	0.43
M6	4.6	2.2	6.8	0.4	ND	0.40
M7	ND	4.6	4.6	0.36	ND	0.36
M8[2]	ND	ND	ND	*Co-eluted with M3*		

ND, not detected.

The relative abundance of metabolites is based on the amount of radioactivity excreted in urine and feces.

1. Metabolite M4 co-eluted with M2 but was a minor component of the peak (Figure 2).

2. Metabolite M8 co-eluted with M3. The amount of M8 could not be assessed (Figure 4).

Figure 1

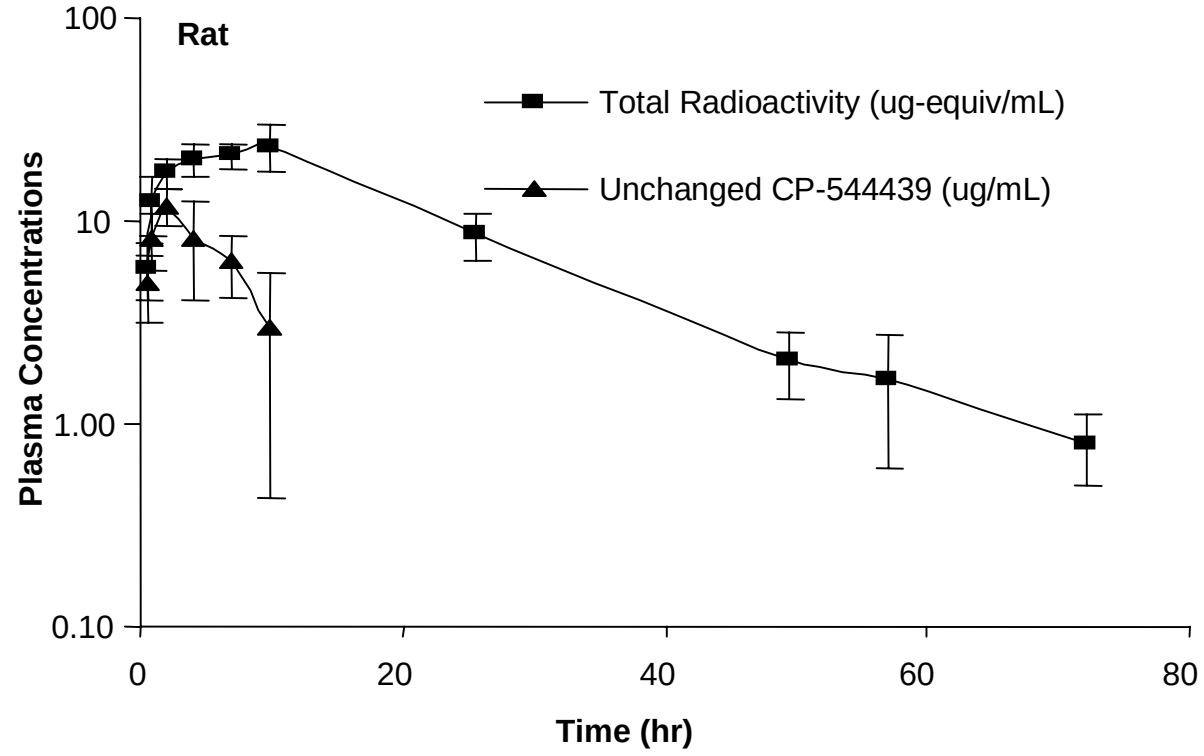

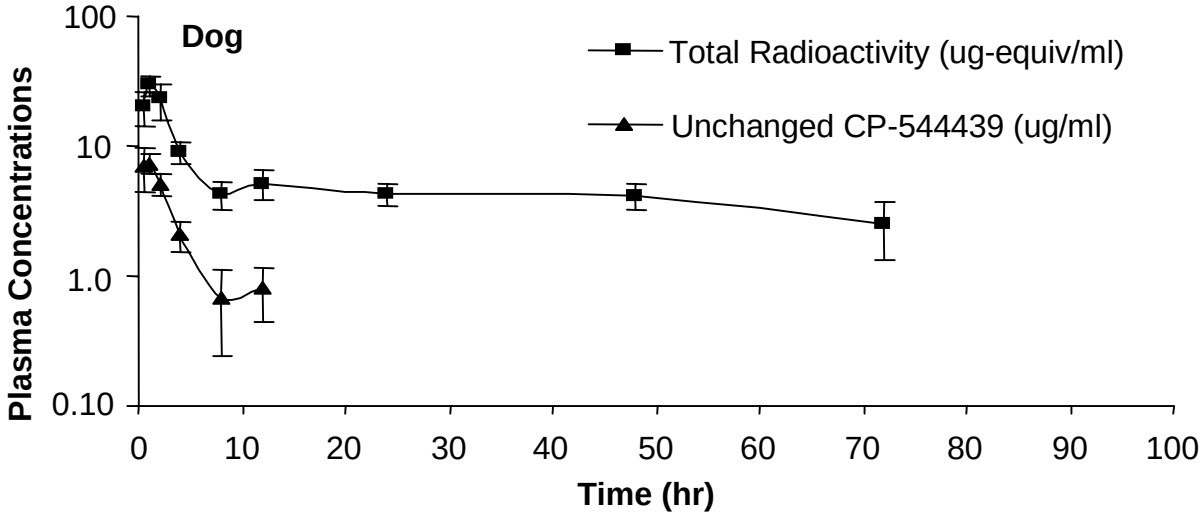

Figure 2AB

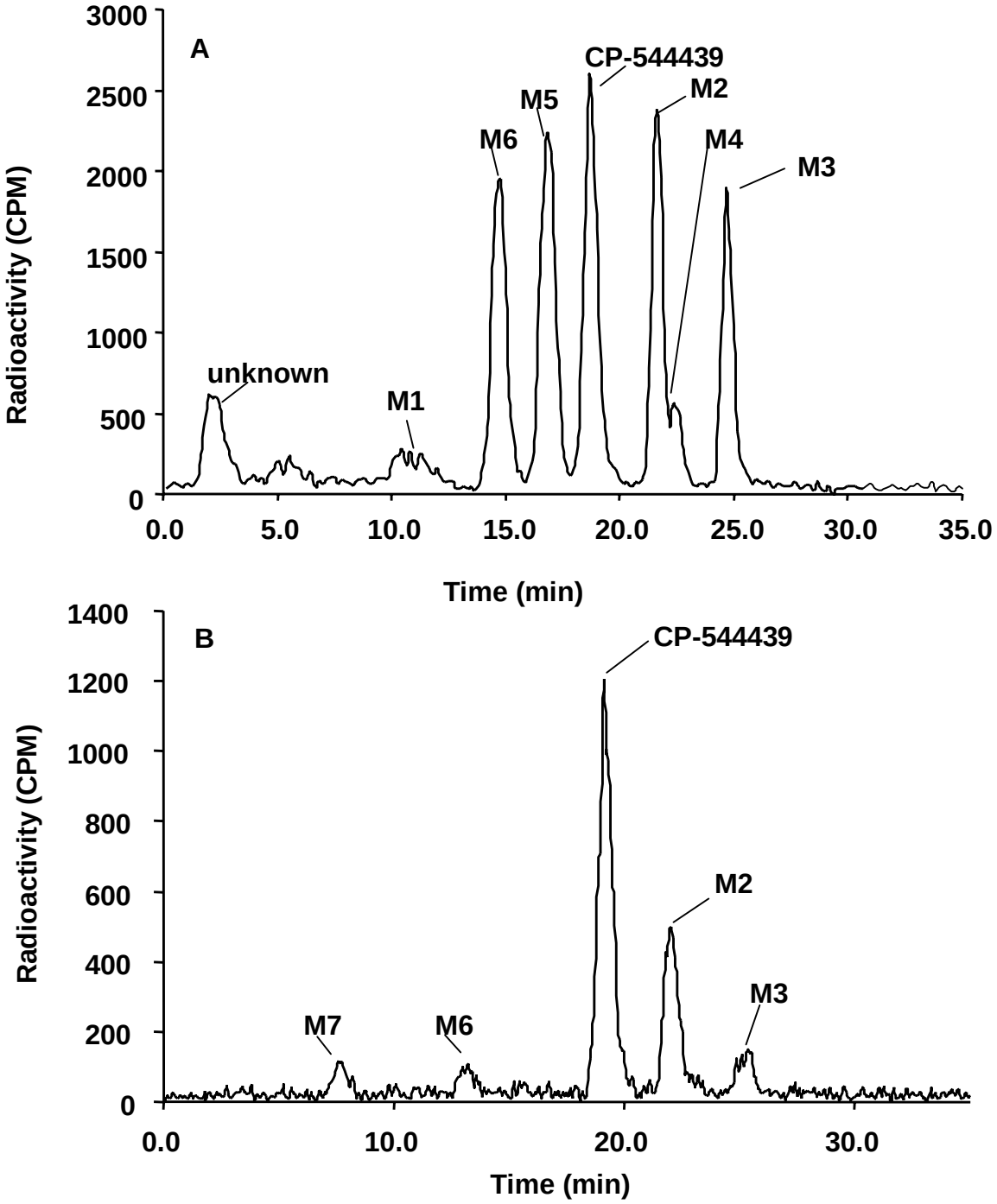

Figure 3

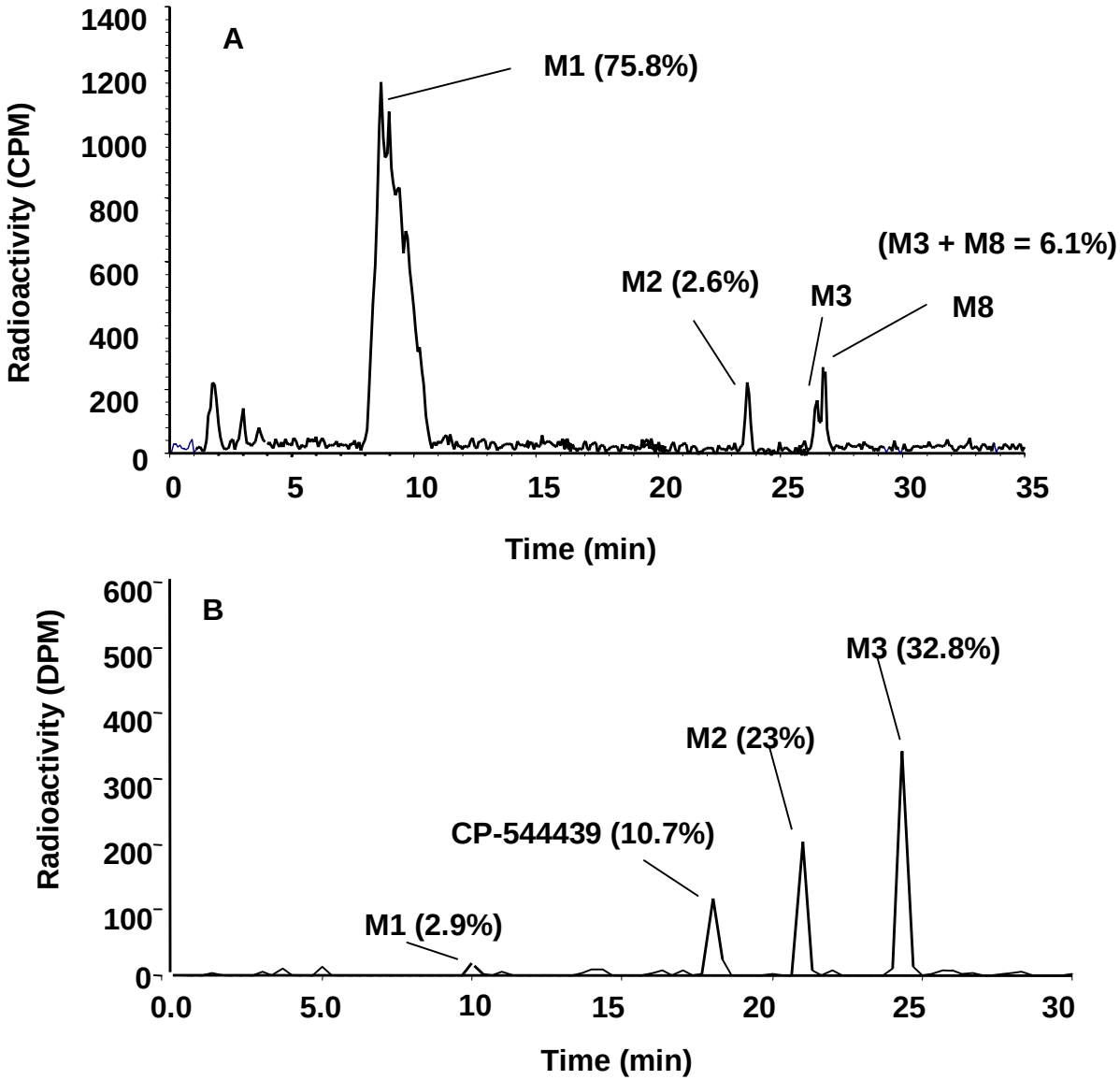

Figure 4

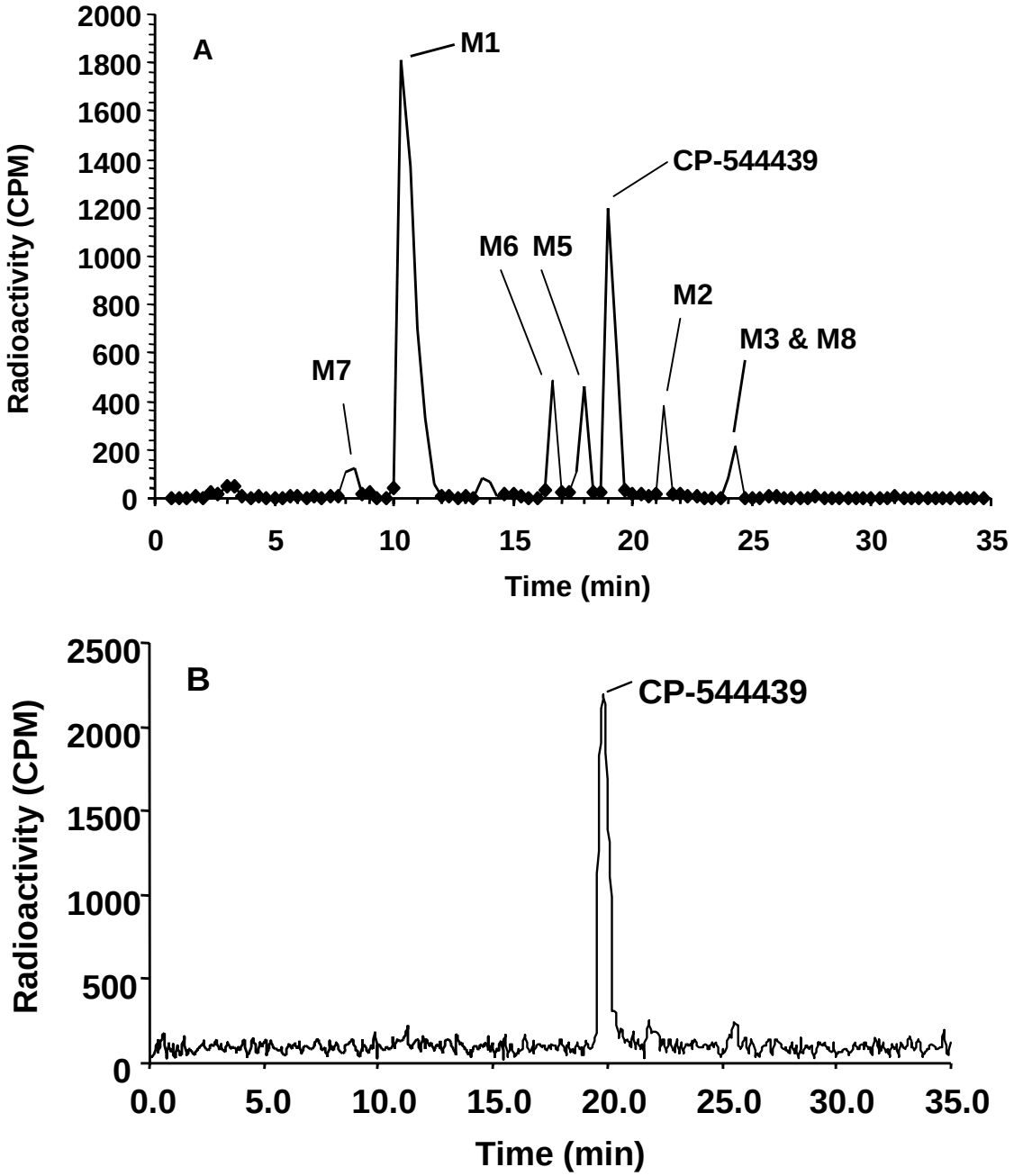

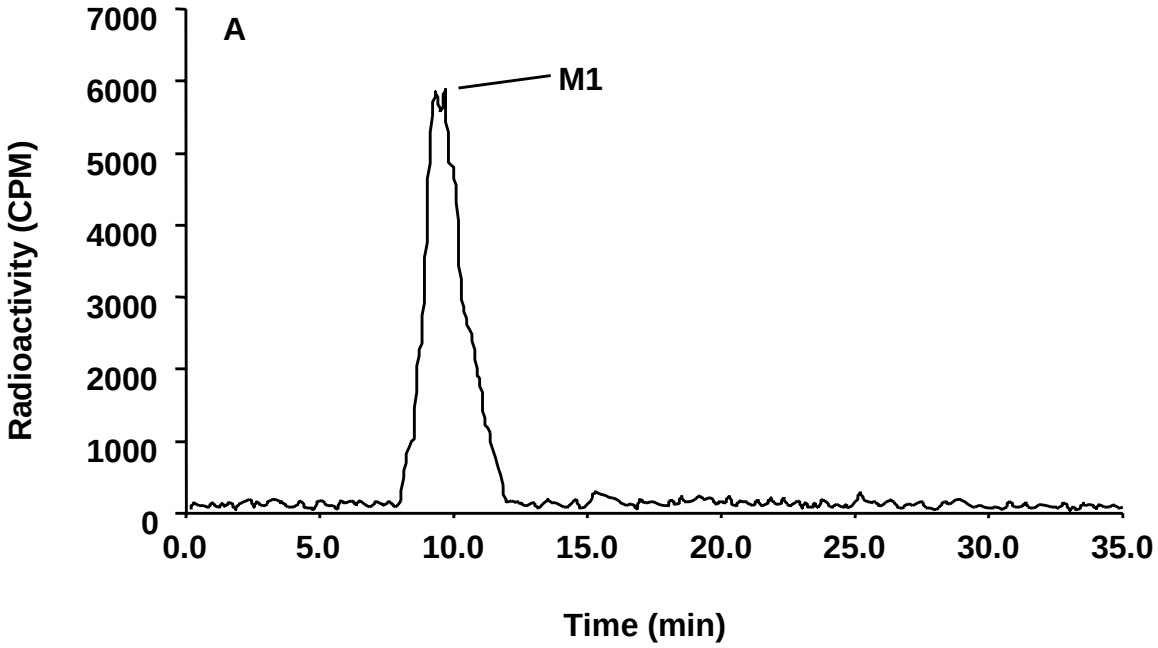

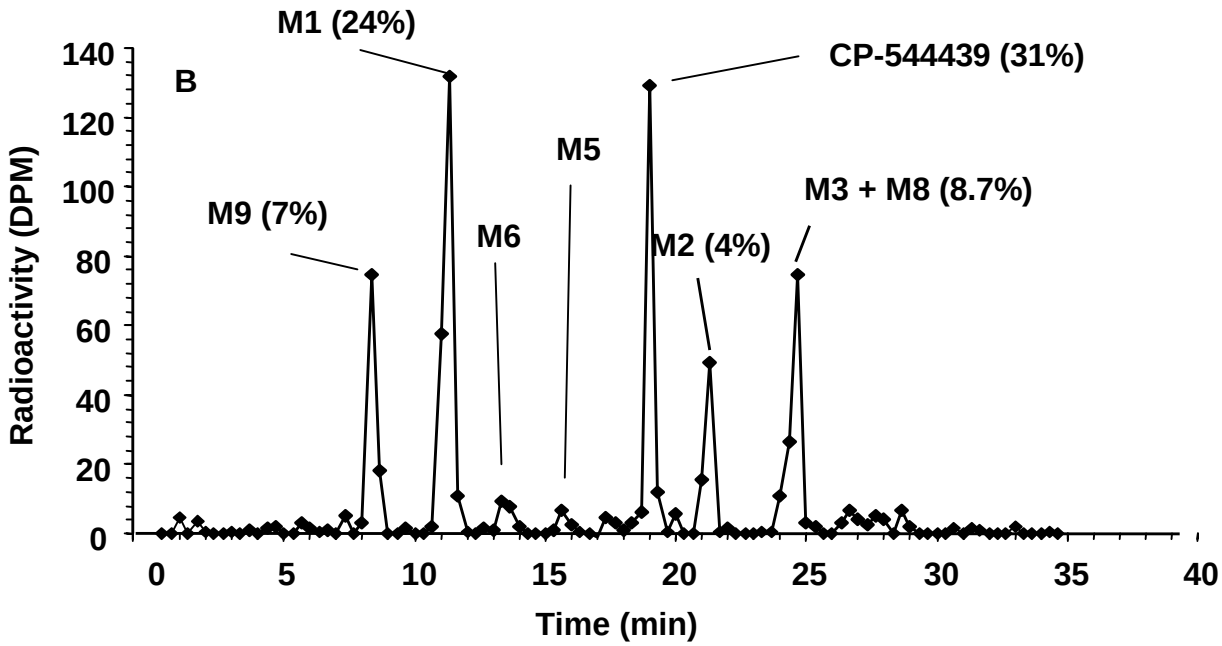

Figure 5

Figure 6

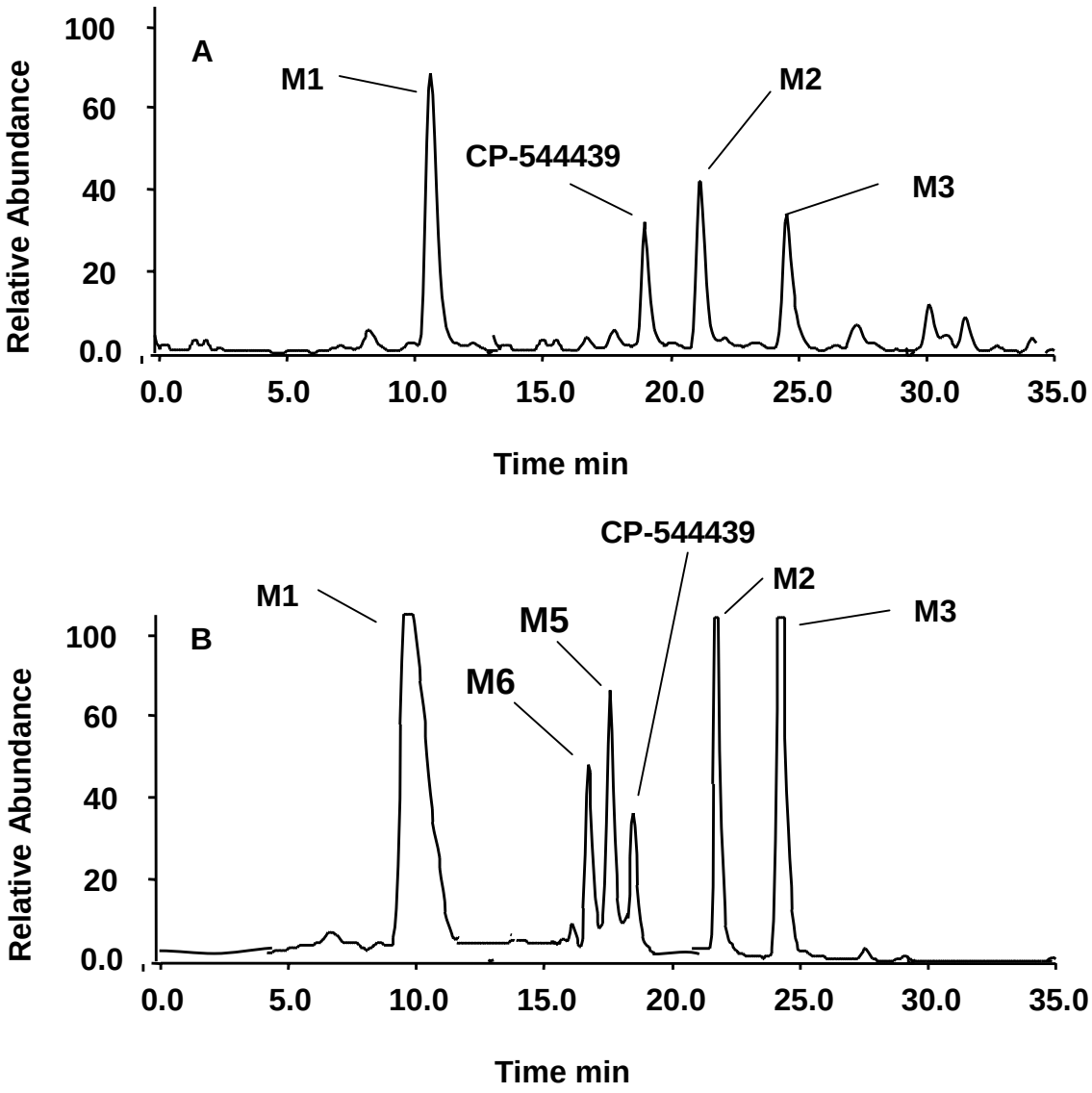

Figure 7

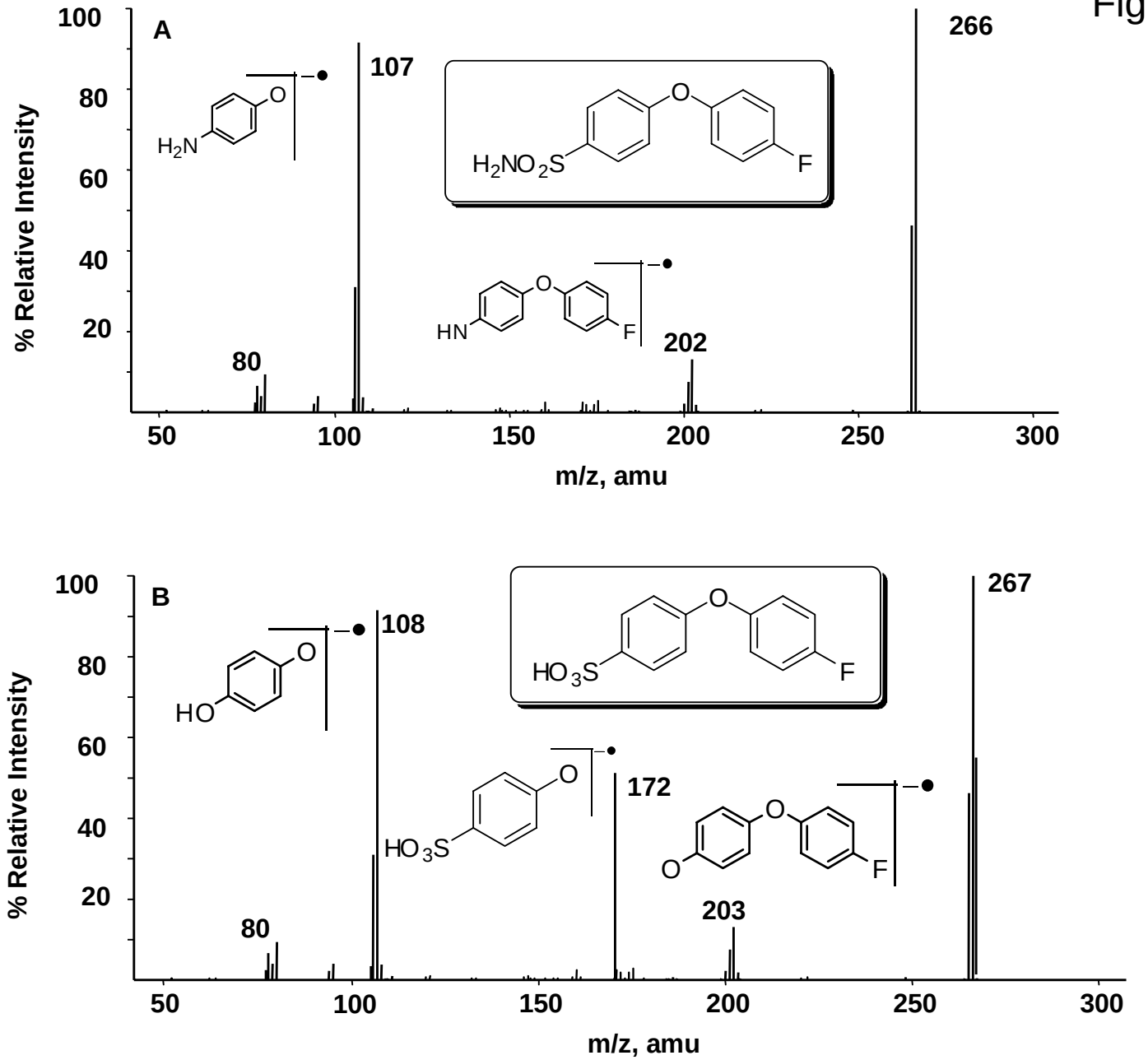

Figure 8